Development of the Next Generation Metro-Wide Simulation Models for the Twin Cities' Metropolitan Area: Mesoscopic Modeling

Final Report

Prepared by:

Henry X. Liu
Adam Danczyk
Xiaozheng He

Department of Civil Engineering
University of Minnesota

CTS 11-03

Technical Report Documentation Page

1. Report No.	2.	3. Recipients Accession No.	
CTS 11-03			
4. Title and Subtitle Development of the Next Generation Metro-Wide Simulation Models for the Twin Cities' Metropolitan Area: Mesoscopic Modeling		5. Report Date January 2011 6.	
7. Author(s) Henry X. Liu, Adam Danczyk, and Xiaozheng He		8. Performing Organization Report No.	
9. Performing Organization Name and Address Department of Civil Engineering University of Minnesota 500 Pillsbury Dr. S.E. Minneapolis, MN 55455		10. Project/Task/Work Unit No. CTS Project #2008085 11. Contract (C) or Grant (G) No.	
12. Sponsoring Organization Name and Address Intelligent Transportation Systems Institute Center for Transportation Studies 200 Transportation & Safety Building 511 Washington Ave. SE Minneapolis, MN 55455		13. Type of Report and Period Covered Final Report 14. Sponsoring Agency Code	
15. Supplementary Notes http://www.cts.umn.edu/Publications/ResearchReports/			

16. Abstract (Limit: 250 words)

The collapse of the Interstate 35W Bridge over the Mississippi River in Minneapolis resulted in unexpected loss of life and had serious consequences on mobility and accessibility in the Twin Cities metropolitan area. In response to the network disruption caused by the bridge collapse, a number of traffic restoration projects were proposed and rapidly implemented by Mn/DOT. Selection and prioritization of these projects, however, was based mainly on engineering judgment and experience. The only decision-support tool available to traffic engineers was the regional transportation planning model, which is static in nature and decennial.

In this work, the Twin Cities metropolitan area is simulated using a mesoscopic traffic simulator in the AIMSUN software. After establishing the mesoscopic simulation model, we attempt to utilize the calibrated mesoscopic simulation model to evaluate drivers' perceived cost evolution to explain the traffic dynamics on the Twin Cities road network after the unexpected collapse of the I-35W Bridge over the Mississippi River. Given the observation of largely underutilized sections of network, it is proposed that the tragedy generated a perceived travel cost to discourage commuters from using these sections. Applying a mesoscopic simulation model provided by AIMSUN, the perceived costs on cordon lines after the I-35W Bridge collapse were suggested to be best described as an exponential decay cost curve. The proposed model is applicable to both practitioners and researchers in traffic-related fields by providing an understanding of how traffic dynamics will evolve after a long-term, unexpected network disruption.

17. Document Analysis/Descriptors	18. Availability Statement		
I-35W Mississippi River Bridge, Bridges, Collapse, Mesoscopic traffic simulation, Mesoscopic traffic flow, AIMSUN	No restrictions. Document available from: National Technical Information Services, Springfield, Virginia 22161		
19. Security Class (this report) Unclassified	20. Security Class (this page) Unclassified	21. No. of Pages 55	22. Price

Development of the Next Generation Metro-Wide Simulation Models for the Twin Cities' Metropolitan Area: Mesoscopic Modeling

Final Report

Prepared by:

Henry X. Liu
Adam Danczyk
Xiaozheng He

Department of Civil Engineering
University of Minnesota

January 2011

Published by:

Intelligent Transportation Systems Institute
Center for Transportation Studies
200 Transportation & Safety Building
511 Washington Avenue SE
Minneapolis, Minnesota 55455

The contents of this report reflect the views of the authors, who are responsible for the facts and the accuracy of the information presented herein. This document is disseminated under the sponsorship of the Department of Transportation University Transportation Centers Program, in the interest of information exchange. The U.S. Government assumes no liability for the contents or use thereof. This report does not necessarily reflect the official views or policies of the University of Minnesota.

The authors, the University of Minnesota, and the U.S. Government do not endorse products or manufacturers. Any trade or manufacturers' names that may appear herein do so solely because they are considered essential to this report.

Acknowledgements

The author(s) wish to acknowledge those who made this research possible. The study was funded by the Intelligent Transportation Systems (ITS) Institute, a program of the University of Minnesota's Center for Transportation Studies (CTS). Financial support was provided by the United States Department of Transportation's Research and Innovative Technologies Administration (RITA).

Table of Contents

1 Introduction 1
2 Mesoscopic Simulation Tool 3
3 Simulation Process 5
3.1 Network Representation 5
3.2 Traffic Modeling 5
3.2.1 Traffic Demand Data 6
3.2.2 Vehicle Entrance Process 6
3.2.3 Vehicle Movement 6
3.2.4 Node Model 6
3.3 Global Modeling Parameters 7
4 Building the Model 9
4.1 Data Preparation 9
4.1.1 Base Map 9
4.1.2 Traffic Control 12
4.1.3 Origin-Destination Demand 13
4.1.4 Loop Detector Data for Calibration Effort 15
4.2 Model Calibration 16
4.2.1 Capacity Calibration 16
4.2.2 Demand Calibration 17
4.2.3 Calibration Targets 24
4.3 Calibration Results 25
4.3.1 Criteria #1: Traffic Counts 25
4.3.2 Criteria #2: Speeds 28
4.3.3 Criteria #3: Queue Formation 31
5 Applications of Mesoscopic Simulation Model 33
5.1 Network Performance Changes after the I-35W Bridge Collapse/Reopening 33
5.2 Perceived Cost Model Development 33
6 Conclusions 43
7 Future Research 45
7.1 Integration with Microscopic Traffic Simulation Model 45
7.2 Integration with Day-to-Day Learning Process 45
References 47

List of Figures

Figure 1: Road map of the Twin Cities network 10
Figure 2: GIS Map of Twin Cities conflated network 11
Figure 3: Final network topology 12
Figure 4: TAZs in Downtown Minneapolis 14
Figure 5: Simplified SuperTAZ in Downtown Minneapolis 14
Figure 6: Twin Cities loop detectors used in the network (green dots) 16
Figure 7: Deleting internal SuperTAZ trips 18
Figure 8: SuperTAZs with neighbors connected via local streets 19
Figure 9: Procedure for OD matrix update 22
Figure 10: A corridor with observations that require trip demand matrix adjustment. Blue circles represent loop detector sites and three interchanges are present, each with their own demand 23
Figure 11: Daily trips entering the Twin Cities freeway network via on-ramps 34
Figure 12: Five cordon circles around the Twin Cities 35
Figure 13: Total traffic counts for each cordon circle 37
Figure 14: Time-based toll costs, as computed in the Twin Cities model 39
Figure 15: Exponential decay curves for given cordons 40

List of Tables

Table 1: Example of acceptance criteria 24
Table 2: GEH statistics for 1st set of loop detectors 26
Table 3: GEH statistics for 2nd set of loop detectors 27
Table 4: Relative error for speed of 1st set of loop detectors 29
Table 5: Relative error for speed of 2nd set of loop detectors 30
Table 6: Network-level performance measures before and after bridge collapse 33
Table 7: Network topologic features of cordoned areas 36
Table 8: Coefficient values for cordon circles 40
Table 9: Simulated and observed flows on a week-by-week basis following I-35W bridge collapse, along with the corresponding GEH statistic 42

Executive Summary

The collapse of the Interstate 35W Bridge over the Mississippi River in Minneapolis resulted in unexpected loss of life and had serious consequences on mobility and accessibility in the Twin Cities metropolitan area. In response to the network disruption caused by the bridge collapse, a number of traffic restoration projects were proposed and rapidly implemented by Mn/DOT. Selection and prioritization of these projects, however, was based mainly on engineering judgment and experience. The only decision-support tool available to traffic engineers was the regional transportation planning model, which is static in nature and decennial. Although such a model is suitable for the evaluation of long-term (on the order of five years or longer) transportation investments, it is not appropriate or adequate for short-term (within days or weeks) operational planning in response to a disaster or other emergencies. This is partly because the macro model neither takes into account temporal and spatial changes in the origin/destination information, nor does it capture the effect of traffic control. In particular, affected travelers need to explore new routes and destinations on a daily basis after network disruption; prioritization of transportation projects will need to take travelers' day-to-day learning processes into consideration. There is therefore a strong need for a region-wide simulation tool that can be used to evaluate the effectiveness of temporary traffic restoration projects as well as other emergencies and rapid response to on-demand planning needs, some of which are dictated by political or budget needs.

Simulating traffic in a large metropolitan area, in the past, has been a very difficult endeavor. Traditionally, two types of simulation software have been available: macroscopic and microscopic traffic simulation. While microscopic, which focuses on the finer details of traffic dynamics, is regarded as “more realistic representation” if calibrated correctly, the calibration endeavor is time-consuming and difficult, especially on large networks. Macroscopic, however, is generally considered too broad and best used to determine rough estimates of traffic performance. Recently, mesoscopic traffic simulation, which is situated between both microscopic and macroscopic in terms of detail, has become available in commercial transportation software. In general, mesoscopic models describe the traffic entities at a high level of detail, but individual travel choices are described at a lower level of detail.

In this work, the Twin Cities metropolitan area is simulated using a mesoscopic traffic simulator in the AIMSUN software. This large-scale network includes all major freeways, major arterials, and other roads that exceed a level of importance deemed by the modeler. Using a planning origin-destination matrix, demands throughout the network were calibrated for July 2007 so that a set of practice-defined calibration targets were met. The calibrated mesoscopic simulation model serves as a guidance tool for scenario testing and offers help to provide some preliminary answers to research questions that arise in a wide variety of areas.

After establishing the mesoscopic simulation model, we attempt to utilize the calibrated mesoscopic simulation model to evaluate drivers’ perceived cost evolution to explain the traffic dynamics on the Twin Cities road network after the unexpected collapse of the I-35W Bridge over the Mississippi River. Based on the loop detector data, we observe an avoidance phenomenon, where demand in areas near the bridge drastically drops following collapse and gradually recovers to pre-collapse demands. Given the observation of largely underutilized

sections of network, it is proposed that the tragedy generated a perceived travel cost to discourage commuters from using these sections. Applying a mesoscopic simulation model provided by AIMSUN, the perceived costs on cordon lines after the I-35W Bridge collapse were suggested to be best described as an exponential decay cost curve. After reinstituting this calibrated cost curve into the mesoscopic traffic simulator, the simulated demands into the discouraged areas are generated within acceptable limits of the observed demands on a week-by-week basis. The proposed model is applicable to both practitioners and researchers in traffic-related fields by providing an understanding of how traffic dynamics will evolve after a long-term, unexpected network disruption.

In addition to studying the traffic evolution after unexpected network disruption, several other research applications as well as potential uses for the calibrated simulation model are outlined and recommended. This model will effectively serve as a useful tool to generate data necessary for future research projects, particularly in regard to the unexpected link closure and reopening.

1 Introduction

Simulating traffic in a large metropolitan area has, in the past, been a very difficult endeavor. Traditionally, two types of popular simulation software have been available to offer assistance. The first type, known as macroscopic traffic simulation, simulates traffic flow dynamics with macroscopic flow conservation equation and the fundamental relationships between the three main traffic flow parameters—speed, flow, and density. However, this model suffers from a lack of realism, as both strategic travel decisions (such as route choice) and tactical driving decisions (such as lane-changing and gap-acceptance) have historically not been incorporated into this type of simulation. The second type, known as microscopic traffic simulation, simulates traffic demand by modeling individual vehicles as they move through the network. Both strategic travel decisions and tactical driving decisions are considered in microscopic simulation. Simulated vehicles are influenced by one another and are governed by a set of rules in terms of how to behave when given a dilemma, such as changing lanes or overtaking another vehicle. While extremely assistive to small-scale problem such as intersection design, the computational demand for microscopic simulation often renders it impossible to use on large-scale networks.

A third type of traffic simulation called mesoscopic traffic simulation has become more and more popular in recent years. Mesoscopic traffic simulation essentially falls between macroscopic and microscopic traffic simulation, in terms of level of detail. Generally, in mesoscopic traffic simulation, while individual vehicles are simulated with some strategic travel decisions (such as route choice), the tactical driving behavioral models are simplified and more closely related to macroscopic traffic flow relationship. Mesoscopic simulation strikes a balance between the two by offering more accurate detail than macroscopic, but by requiring less computation time than microscopic.

Existing mesoscopic models describe traffic using various approaches. One specific approach, such as CONTRAM (Leonard et al., 1989), is to group vehicles into packets to travel through the network. The speed of each packet of vehicles is derived from a speed-density relationship defined for each link. The lane changes and acceleration/deceleration of vehicles are not modeled in this approach. Another mesoscopic model, DYNASMART (Jayakrishnan et al., 1994), uses a queue-server approach to describe traffic transition. In the model, vehicles traverse the running part of a link with a speed that is determined using a macroscopic speed-density relationship; and at the downstream end, a queue-server transfers vehicles to connecting links. DYNAMIT (Ben-Akiva et al., 1997) applies an alternative approach in which vehicles are traveling as groups of cells. Although vehicles can enter and leave cells when needed, their behavior is controlled by cells, not the individual drivers' decisions. Cellular automata is another approach used by other mesoscopic simulation models, e.g., TRANSIMS (Bush, 2000).

In this work, AIMSUN is used to create a traffic simulation model of the Twin Cities metropolitan area. AIMSUN, produced by TSS-Transport Simulation Systems, is one of the many software packages that now include mesoscopic traffic simulation tools. The mesoscopic simulation approach provided by AIMSUM is an event-based simulator. Each node in the simulation works as a queue server and vehicle movements through sections/lanes are modeled as a simplification of the car-following, lane changing, and gap-acceptance models used in the

microscopic approach (see details in Chapter 14, Microsimulator and Mesosimulator in AIMSUN 6.1 User's Manual, 2009).

The goal of this work is to produce a model that can aid in future research studies on the topic of unexpected network disruption. The objectives of this study are (1) to investigate the performance of mesoscopic simulation on the Twin Cities metropolitan network; (2) to replicate the traffic evolution after unexpected network disruption by using the calibrated mesoscopic simulation model. In particular, this research would offer assistance in studying traffic dynamics following the collapse of the I-35W Bridge in August 2007, but the opportunities for other topics, such as traffic evolution after planned road closure, would be certainly available.

This report discusses mesoscopic traffic simulation in AIMSUN, detailing on the exact particulars in how traffic is simulated. From there, it describes the construction of the model and a procedure used to for demand calibration. Using the calibrated Twin Cities' network model, we conduct analysis on the day-to-day traffic dynamic after the I-35 Mississippi River Bridge collapse and reopening. By applying the calibrated mesoscopic simulation model, we replicate the zone avoidance phenomenon observed after the collapse of I-35W Bridge, by introducing additional perceived costs into drivers' perception. Finally conclusion remarks are offered on the simulation and potential integration of the Twin Cities microscopic freeway simulation model.

2 Mesoscopic Simulation Tool

The simulation tool used in this work is AIMSUN 6.0.1. This tool expands existing features provided by earlier versions as well as expands the modeling environment into new areas. The single software application provides models for the traditional travel demand models and microscopic simulation. Additionally, a new mesoscopic traffic simulation component has been added, allowing for the modeling of larger scale networks without the tedious calibration effort required for microscopic simulation. This feature now is available in the AIMSUN program, allowing users familiar with earlier versions of the software an easy opportunity to become familiar with the mesoscopic simulation components.

Mesoscopic simulation has appeal for the Twin Cities model. Given the sizeable area of the Twin Cities network, a microscopic simulation would be too detailed and, thus, very difficult to calibrate. Additionally, given the detailed simulation of individual driver-vehicle units, the time required to produce the desired results would be too excessive. A macroscopic simulation, which bases on link performance functions, would not be to the desired level of accuracy. Macroscopic simulation, which is often used for planning networks, does not model vehicle dynamics, which comes with a loss of realism. Mesoscopic simulation, being situated between macroscopic and microscopic in terms of level of detail, is thus ideal by capturing greater detail than the broad macroscopic simulations, but not being too difficult to calibrate or time-consuming as microscopic simulations.

Currently, the standard of ‘what is mesoscopic simulation’ has not been agreed upon. As a result, several software packages have been developed that run mesoscopic simulation, but the simulation itself is slightly different from its counterparts. These differences appear in several different areas of the simulation component itself. These areas include:

- Simulation Process
- Network Representation
- Traffic Modeling
- Global Parameters

The techniques AIMSUN uses for mesoscopic simulation in these four areas are outlined in later sections.

3 Simulation Process

According to the AIMSUN user manual, the mesoscopic simulation approach is based on a discrete-event simulation, where simulation time may change at non-uniform intervals. Time changes are governed by when certain predefined events occur that change the state of the traffic network. These events include:

- Vehicle Generation
- Vehicle System Entrance
- Vehicle Node Movement
- Change in Traffic Light
- Statistics Generation
- Change in Demand Matrix

A simplification of the car-following, lane changing, and gap acceptance, relative to those used in microscopic simulation, are used to describe vehicle movements during these events. All of the events encountered in AIMSUN are given a time and priority so that the event list may be correctly sorted. For example, a traffic light changing from red to green would be dictated as of higher priority than collecting statistics in the same time interval. For greater detail on the components of discrete-event simulation in AIMSUN, please refer to the user manual.

3.1 Network Representation

AIMSUN defines the network in mesoscopic simulation to be based on a directed graph designed from a simple node-section representation. This directed graph is composed of three basic geometric elements:

- **Nodes**: Node serves where vehicles are transferred from a section to a turning and onwards to the next desired section. These exchanges involve turnings, which are defined connections that vehicles follow from the origin zone to destination zone. Vehicle using these connections are assumed to be moving at free flow speeds.
- **Sections**: Connections between nodes with unique geometries, speed limits, jam densities, and reaction time factors.
- **Centroids**: Sources where vehicles are generated.

The network may also include a series of dummy objects, which are objects necessary for the correct function of the simulation but are not identified as in the AIMSUN network. Such dummy objects would include connections from centroids to real network sections or nodes. Statistical data for these dummy objects are not collected.

3.2 Traffic Modeling

In addition to the discrete-event simulation, one major difference of mesoscopic traffic simulation from microscopic traffic simulation is the simplification of vehicle dynamics and network movement. Car-following, lane changing, and gap acceptance behaviors are simulated with simplifications, which are consistent with macroscopic traffic flow relationships.

3.2.1 Traffic Demand Data

For mesoscopic simulation, origin-destination matrices are used to produce the routes or paths. These matrices require a vehicle type and a simulation time frame. They are very similar to matrices defined for microscopic traffic simulation.

3.2.2 Vehicle Entrance Process

The traffic generation process in AIMSUN produces headway times for each vehicle, which are then used to generate vehicles intended to enter the Dynamic Network Loading. Origin centroids serve as locations for which vehicles enter the network, given that these centroids are connected to the network. The vehicle first uses a virtual section when entering, where a node server holds the vehicle there until a space in the network becomes available. Once the vehicle reaches a real section, it is considered in the network.

3.2.3 Vehicle Movement

Vehicle movement is modeled differently depending on whether the vehicle is in a section or a node. If the vehicle is in a section, a simplified car-following and lane-changing model is applied. If the vehicle is in a node, a gap-acceptance and lane-selection model is applied in addition to the free-flow movement in turnings. The gap-acceptance model applies for when the vehicle is moving from a section to a turning and the lane-selection model applies when the vehicle is moving from a turning to a section.

In mesoscopic simulation, sections and turnings are considered vehicle containers with a maximum storage capacity. This storage capacity can be found for either sections or turnings with knowledge of the jam density, length, and number of lanes. With knowledge of the number of vehicles stored along sections, car-following models and lane-changing models can be applied to calculate section travel time.

3.2.4 Node Model

When a vehicle reaches the end of a section and desires to enter a node, a gap-acceptance model is required to identify when a vehicle may enter. The model used in mesoscopic simulation is a simplification of the one used in microscopic simulation by only taking into account the time for both vehicles to the collision point and the time needed to clear the node or intersection. Once a vehicle has entered a node, it assumes a free flow state along its desired turning. Upon exiting to a new section, the server is required to calculate when it can enter the section and a lane-selection model is used. The mesoscopic lane-selection model differs from the microscopic version by allowing a lane selection to choose the best entrance lane for a section rather than only focusing on a subset of all destinations. Additionally, a look-ahead model included in the AIMSUN mesoscopic simulator aids in lane selection, although this model is the same as the microscopic version.

3.3 Global Modeling Parameters

Of all available global modeling parameters, the only one available for adjustment is the driver's reaction time. Adjusting this reaction time will influence the results of the car-following model. Reaction time is available to be fixed or variable, the difference being the opportunity to define a discrete probability function for each vehicle type.

4 Building the Model

Producing an accurate model to describe Twin Cities traffic in mesoscopic simulation requires two major efforts: 1.) Data Preparation and 2.) Calibration. For Data Preparation, various sources will be required to complete the model, given the absence of a unified effort to date. The following four data sources are used to produce the base model:

- Base Map/Network Topology
- Traffic control information
- Origin-Destination demand from planning model
- Loop detector data

For the Calibration Effort, two forms of calibration are required to ensure the network is thoroughly correct. The two forms include:

- Capacity Calibration
- Demand Calibration

The calibration targets will be discussed in later sections.

4.1 Data Preparation

4.1.1 Base Map

The intent of this model is to serve as an accurate representation of the Twin Cities network. To better aid the reader in how this network appears, Figure 1 demonstrates major roads in the network.

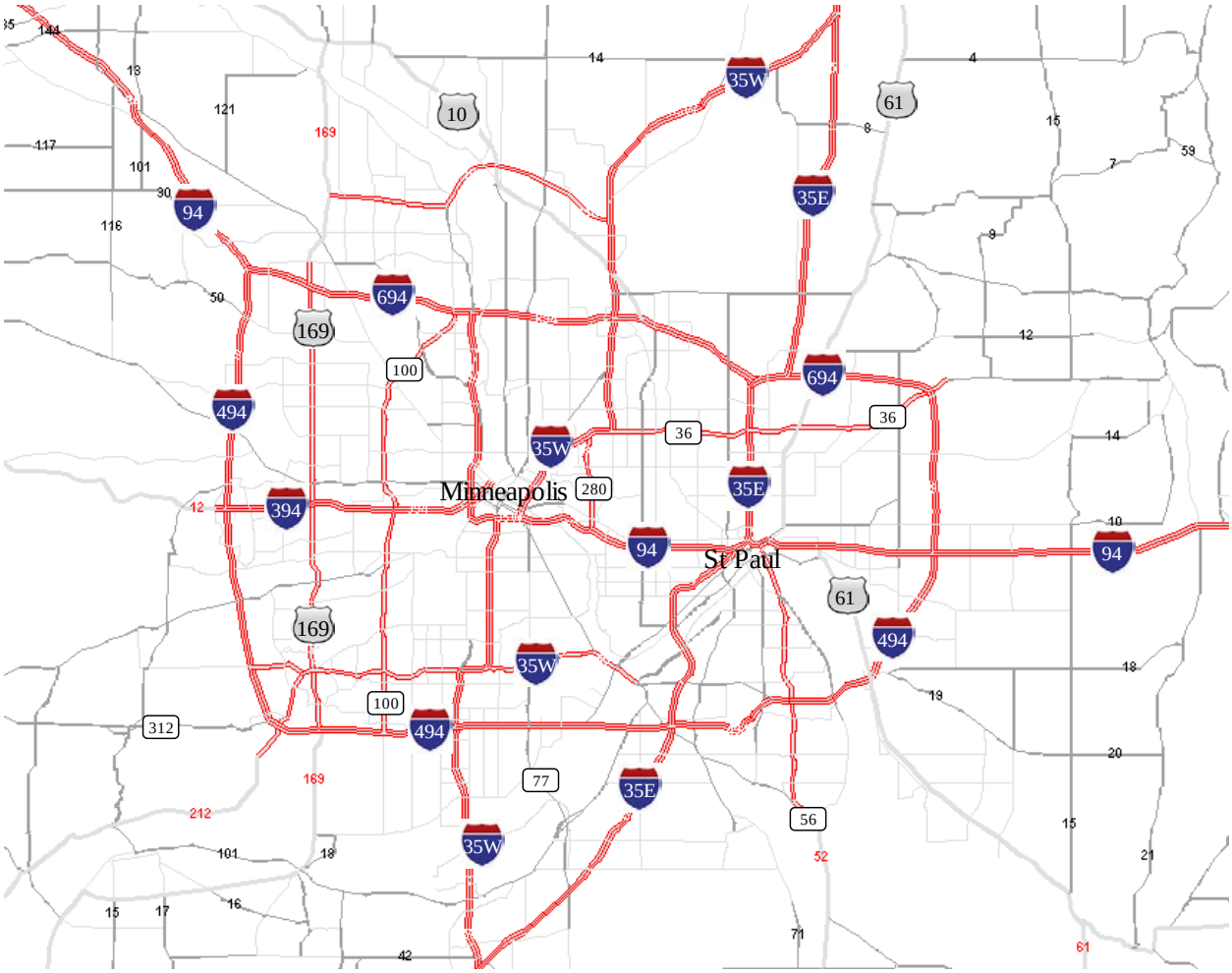

Figure 1: Road map of the Twin Cities network

For a base map, the Twin Cities conflated network was loaded into the AIMSUN program, utilizing the GIS importer available in AIMSUN. Initial loading produced a base map similar to the one in Figure 2. However, this map alone was not operational for several reasons. First and foremost, the translation from GIS to an AIMSUN network resulted in disconnected links at most intersections. Secondly, certain geographic features on non-freeway links were not provided in the GIS file, resulting in many one-lane links with standardized maximum speeds and jam densities. Lastly, some curve data was missing. As a consequence of these facts, the network required some modification.

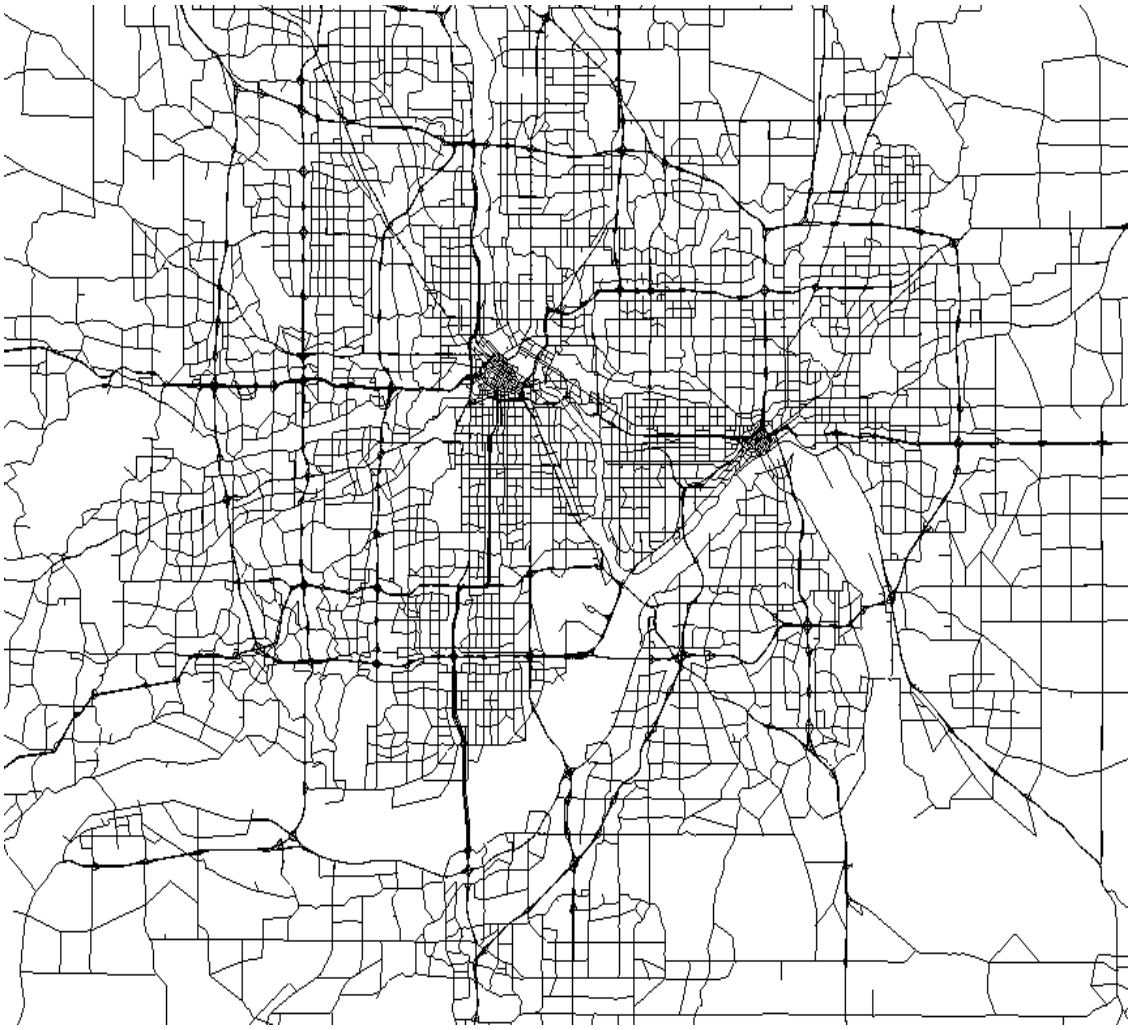

Figure 2: GIS Map of Twin Cities conflated network

While it would be ideal to have more roads to better describe the Twin Cities network, the fixing of so many links would be very time consuming. As a result, it was chosen to instead invest most of the network infrastructure calibration effort on three main types of road:

- Freeways
- Major arterials
- Roads of user-defined importance, based on the modeler's knowledge

When fixing these roads, it was determined to focus on correcting maximum speeds, jam densities, number of lanes, curvature geometries, and intersection geometries. Infrastructure topologies were validated using aerial photography provided by maps.live.com and modeler experience.

The network topology produced following these road definition criteria and calibrated based on data stated above is shown in Figure 3. All other roads included in the original imported network have been removed. In total, there are approximately 630 directional freeway miles present on

the network and 2,400 directional non-freeway (major arterial, minor arterial, user-defined importance, side roads) miles on the network. This produces a ratio of about 1:4.

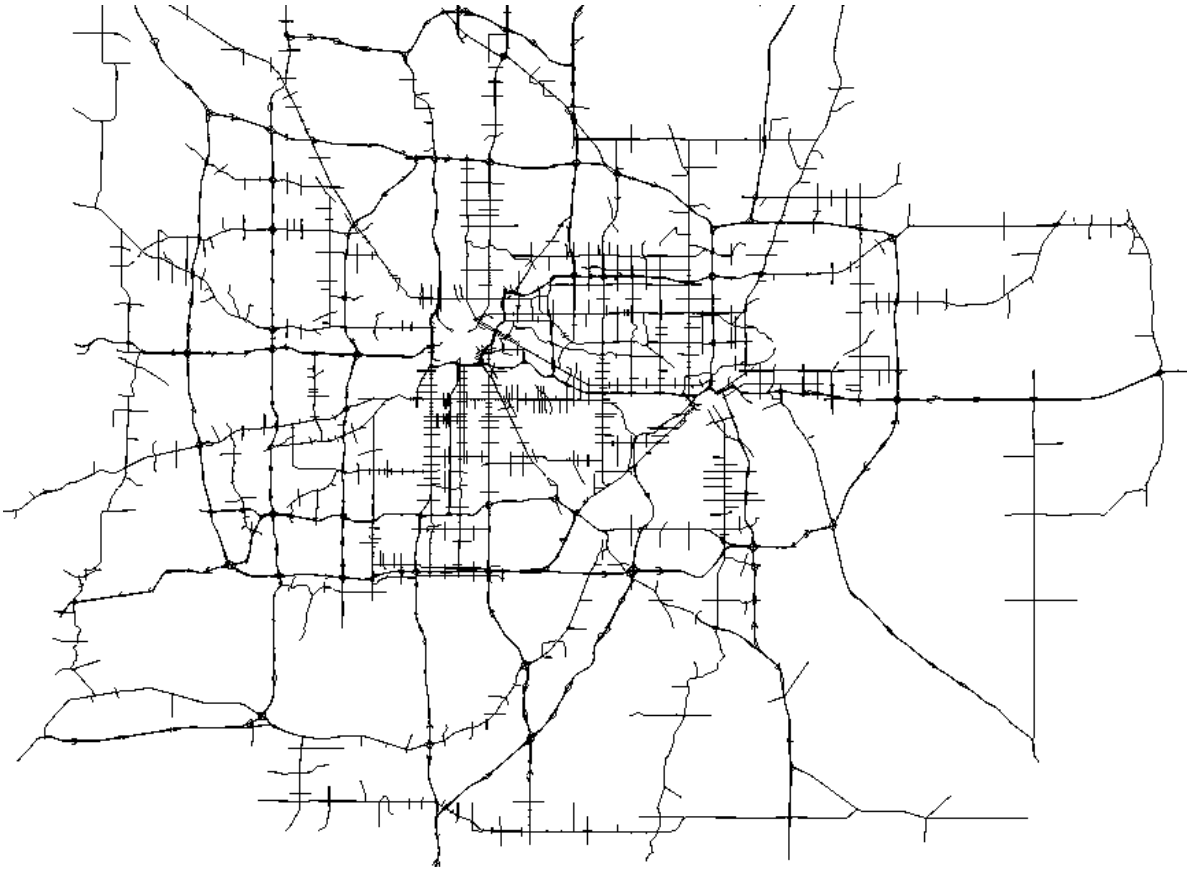

Figure 3: Final network topology

4.1.2 Traffic Control

Given the use of traffic control devices in the real-world, it was deemed prudent to install traffic control devices into the mesoscopic model as well. Unfortunately, this is problematic, as the current version of AIMSUN does not allow for actuated signal control when using mesoscopic traffic simulation. Pre-timed signal is the only available option, which is also problematic in terms of realism when compared with an actuated signal in reality.

To cope with this dilemma, traffic control devices were only deployed in the mesoscopic simulation to major intersections. These major intersections include arterials or important roads that intersect and serve as more than just a collector. For example, the intersection of Central Avenue and Broadway would receive a traffic signal because, in this network, they serve as a through road. All remaining intersections were left as uncontrolled intersections, which were deemed reasonable since a pre-timed signal would likely cause excessive delay if not timed correctly.

When intersections are set as uncontrolled in AIMSUN mesoscopic model, no traffic controls are involved in the discrete event list. For those uncontrolled intersections, vehicle movement from sections to turnings is simulated by applying gap-acceptance model. Vehicle turnings at the uncontrolled intersections are considered without the impact from signals. All vehicles are assumed to travel without any restriction so at a free flow speed in turnings. Finally, vehicle movement from turnings to sections follows a lane selection model.

4.1.3 Origin-Destination Demand

For an initial understanding of Twin Cities traffic demand, the 2007 Twin Cities Trip Matrix from Twin Cities Metropolitan Planning Council was used. This matrix identified more than 1,200 Traffic Analysis Zones (TAZs) around the Twin Cities metropolitan area. Between these TAZs was a given demand generated from a planning model used by the Metropolitan Council. This demand was designed for the peak hour of the AM peak travel period. Given observations from real data around the network, it was assumed this one hour ranged from 8:00 AM to 9:00 AM local time.

Since 1,200 TAZs was deemed excessive for this excercise, these TAZs were simplified to SuperTAZs. Each SuperTAZ consists of a set of smaller TAZs and was intended to reduce extra computing power needed for trips using the local network that was not included in this model. The number of TAZs in a given SuperTAZ vary depending on location in the Twin Cities, but some may hold as many as 25 TAZs.

Figure 4 shows an example of preexisting TAZs in the downtown Minneapolis area. Figure 5 shows how all of these TAZs could be simplified into one SuperTAZ, thus avoiding an excessive number of internal trips.

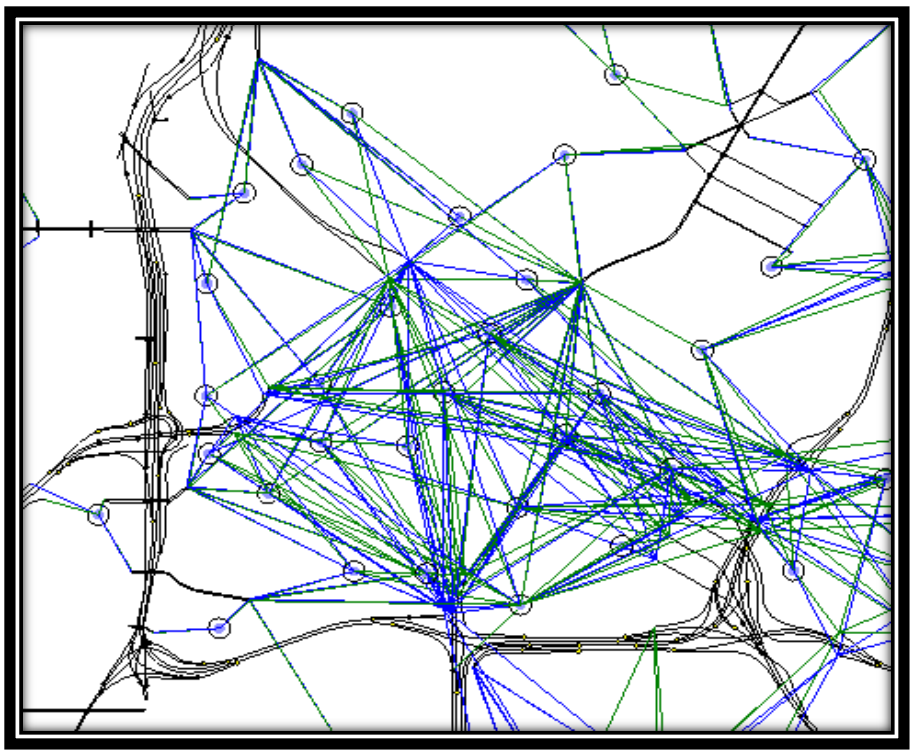

Figure 4: TAZs in Downtown Minneapolis

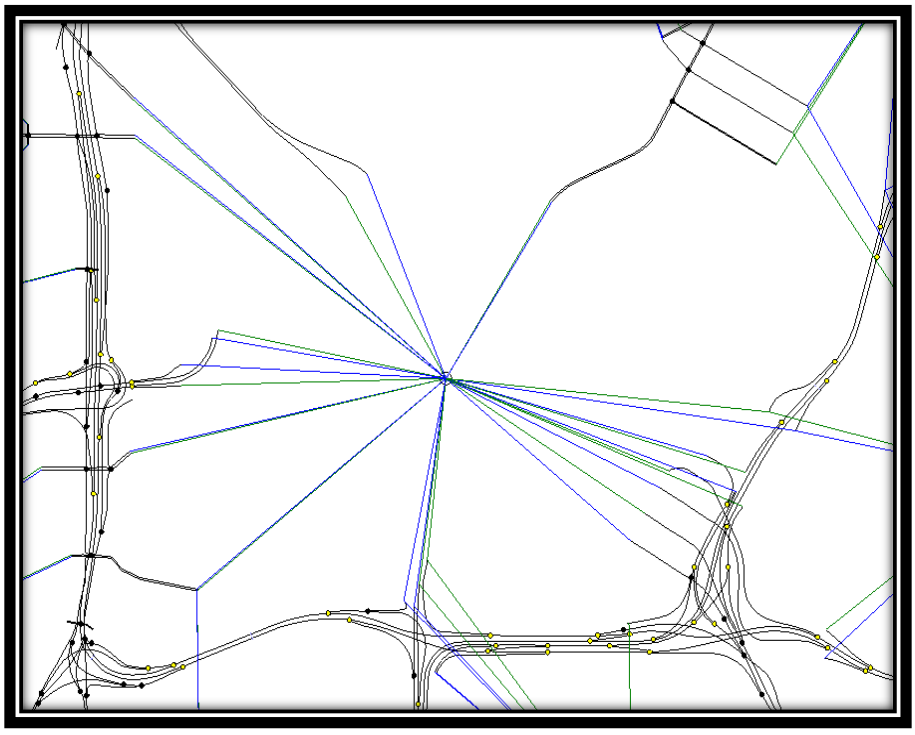

Figure 5: Simplified SuperTAZ in Downtown Minneapolis

For route choice between SuperTAZs, C-Logit assignment was selected. C-Logit, short for Commonality Logit, behaves similar to the Logit function, except discourages selection of alternative routes that overlap with better alternatives. No en-route changes were allowed, as to say that drivers were committed to their chosen routes and did not use external sources to make en-route adjustments. One hour of warm-up time was utilized, as to fill the network with vehicles. Route selection occurred after the warm-up period ended and remained constant during the one hour of traffic simulation.

4.1.4 Loop Detector Data for Calibration Effort

Loop detectors were utilized from the Twin Cities network to aid in the traffic demand calibration effort. These loop detector sites consisted of stations, where loop detectors were allocated to all lanes at a given site as to capture all vehicular traffic passing through the area. We should note that loop detectors were only available on the freeway network, meaning that no data was available for collection along the arterials. Of all the available loop detectors to provide data, 200 – 250 sites were selected (only 200 of these sites were operational). This limited number was intended to allow for an easier, broader calibration effort, where traffic demand traveling between regions could be calibrated instead of calibrating behavior with heavy detail throughout the network. This finer detail was intended to be left for later work.

Figure 6 shows a sample of the selected loop detectors used in this network, where the green dots represent the sites of the loop detector stations.

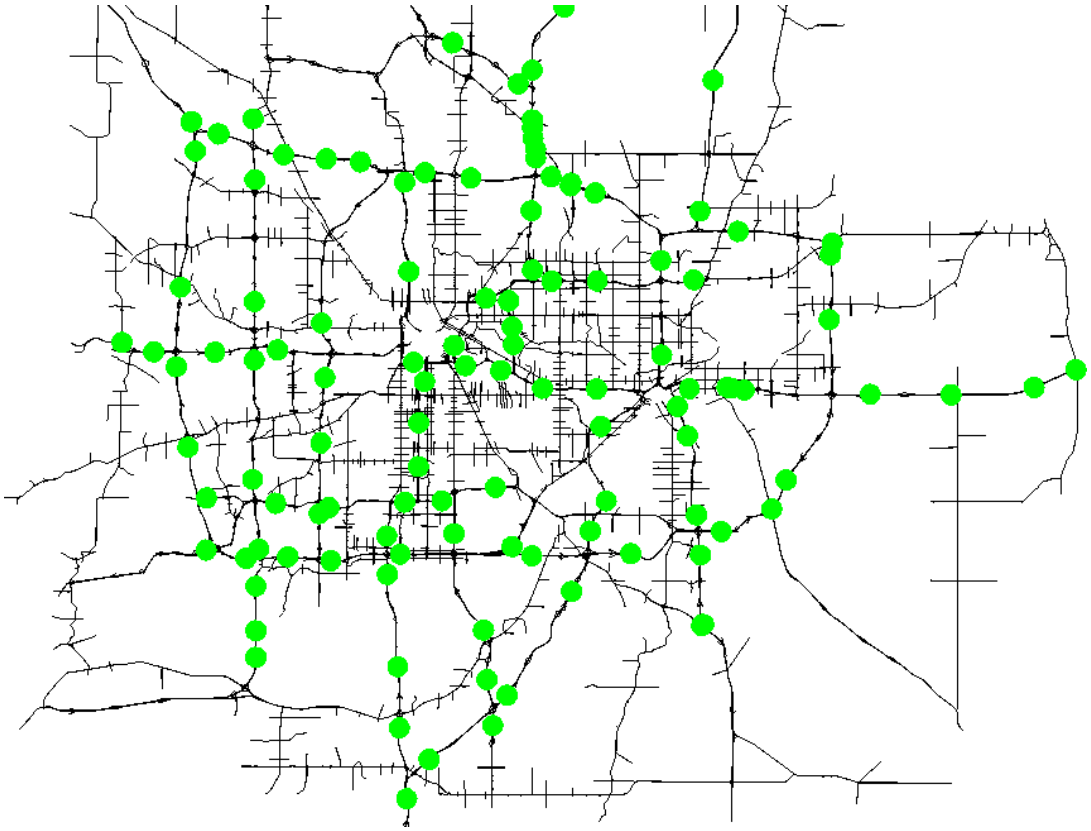

Figure 6: Twin Cities loop detectors used in the network (green dots)

The time period of analysis was selected to be July 25th, 2007, which represented traffic patterns of late July just mere days before the collapse of the I-35W Bridge, which occurred on Aug.1, 2007. July 25th, 2007 was selected after an analysis on the data from the month of July, and considered as a "typical" day in terms of traffic congestion pattern. One-hour data was collected from these detectors, data which includes both count and average speed from 8:00 AM to 9:00 AM that day.

4.2 Model Calibration

4.2.1 Capacity Calibration

Calibrating the capacity in the network follows mostly what is described in the earlier section titled 'Base Map'. Given that many links or nodes in the network are represented incorrectly when we load the GIS file into AIMSUN, each section of road must be investigated to guarantee it represents corresponding sections in reality. Factors to influence include maximum speeds, jam densities, number of lanes, curvature geometries, intersection geometries, and other minor characteristics. Topology of the network was validated using aerial photography provided by maps.live.com and modeler's field observation. Speed limits were set to be consistent with those from the field.

Since the mesoscopic simulator follows discrete-event simulation (Law and Kelton, 1991), traditional flow-density relationship is not used in the model. In the mesoscopic simulation model of AIMSUN, instead, the capacity of a lane denotes the number of vehicles that the lane can hold. To calibrate capacity in the mesoscopic model, the jam density is utilized in addition to the availability of network topology and speed limits. When a lane reaches the jam density, it is considered that the lane is full so no more vehicles can enter the lane until the first vehicle in the lane leaves it. The following jam densities were assigned uniformly to roads throughout the network:

- 210 vehicles/mile/lane for freeways
- 230 vehicles/mile/lane for on-ramps or off-ramps
- 260 vehicles/mile/lane for major arterials or other "surface" roads

The goal of this calibration effort was to make the AIMSUN network as close to reality as possible. This value of closeness was based on the designer's own knowledge of the network infrastructure and observations made through the maps.live.com website. Given the limited amount of data available to provide details on a link-by-link basis, the network infrastructure in the model was deemed sufficiently close to reality.

4.2.2 Demand Calibration

Demand calibration is by far the more time-consuming effort, as numerous iterations are often required to produce a demand matrix that results in realistically modeled traffic. The traditional means to produce a realistic demand matrix is to utilize an existing demand matrix and then make some minor adjustments to refine the accuracy of simulated flow compared with observed flow. This methodology is employed in this work, where the 2007 Twin Cities AM Peak Hourly Trip table discussed in the previous section is used as the base and minor adjustments are made to match observed traffic flow along loop detectors described above.

Given that the design of the network will likely not produce simulated flows from the trip matrix that match those in reality, certain trips will have to be added or removed. To do this while minimizing the impact to the original trip matrix, a three-step process is defined. This three-step process assists in removing excess trips from certain locations while adding necessary trips in other locations. The three steps, followed sequentially, are defined below:

1.) Delete any internal SuperTAZ Demand,
2.) Delete any neighboring SuperTAZ demand where surface streets are likely available,
3.) Adjust corridor travel to be consistent with the loop detector data.

These three steps are outlined in detail below.

Demand Calibration Step 1: Delete Internal SuperTAZ Demand

Since numerous small TAZs were grouped into a single SuperTAZ, there exists local trips that travel within a SuperTAZ. This is problematic because these local trips will be required to enter the AIMSUN network in order to reach their destination again. For example, a car traveling within SuperTAZ #1 will have to leave SuperTAZ #1, travel on a network road, and find a new

access point to reenter SuperTAZ #1. This produces excess travel on the AIMSUN network that, in reality, would have traveled on the local streets within SuperTAZ #1.

Fortunately, this problem is an easy one to fix. All trips traveling with an origin and destination being the same SuperTAZ are set to a default value of zero. Figure 7 shows how this process is done, where the darkened red boxes are locations that are set to zero. As shown, these boxes also represent trip sites traveling within a SuperTAZ.

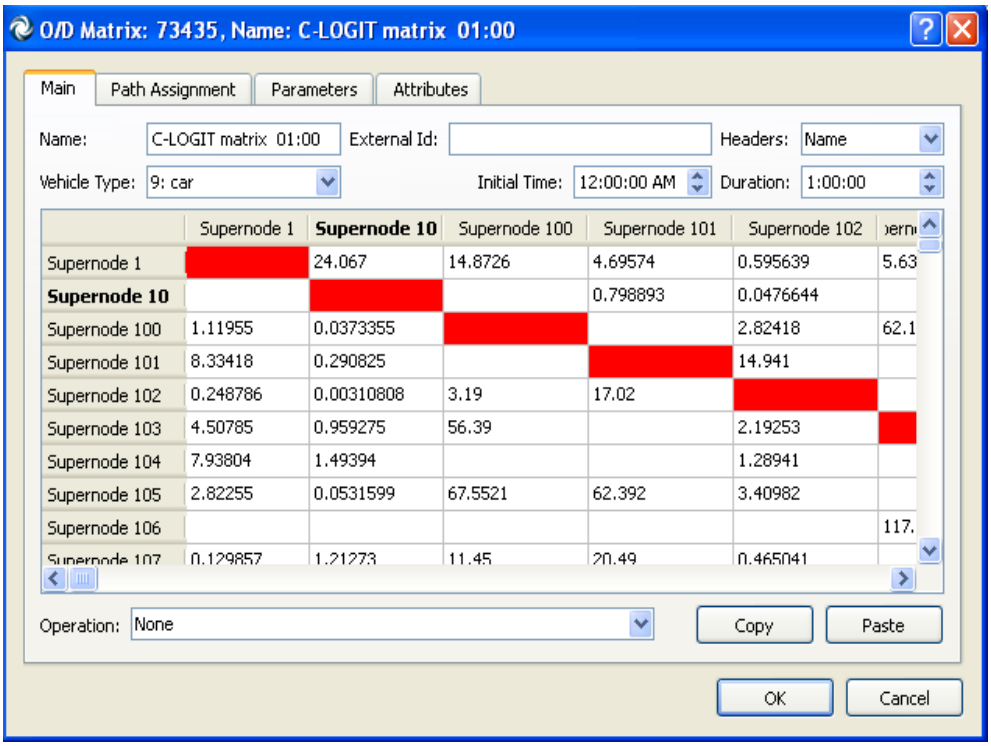

Figure 7: Deleting internal SuperTAZ trips

Demand Calibration Step 2: Delete Neighboring SuperTAZ Demand where surface streets are available

Since many local streets in reality are not accounted for in the model, several SuperTAZs exist that are effectively next to one another and are interconnected via the local streets not included in the model. Without these local streets, demand between these SuperTAZs would be routed to the nearest road and follow a path through the AIMSUN network to the other SuperTAZ. In reality, however, these paths would likely not exist and it is unrealistic to include them in the mode.

To deal with this problem, a qualitative analysis of all SuperTAZs must be conducted. At any given SuperTAZ, the modeler identifies SuperTAZs that are 1.) near the SuperTAZ in question and 2.) likely connected by local roads not provided by the AIMSUN model. Once a pair of SuperTAZs are identified, all demand between them is set to zero, thus deleting unrealistic trips

on the AIMSUN network. Fortunately, this is a simple process as well, but requires a more thorough investigation of all SuperTAZs.

To illustrate this point, Figure 8 shows a series of SuperTAZs that meet these criteria. The SuperTAZs that are red in color can all be considered interconnected with any other red SuperTAZ via local roads. In this particular case, most of these SuperTAZ pairs meet at the entrance and exit ramps. Intuitively, vehicles traveling between these pairs would meet at the exit or entrance ramp and immediately continue via local roads to the other SuperTAZ, as contrast to entering the network, traversing a section, and immediately exiting.

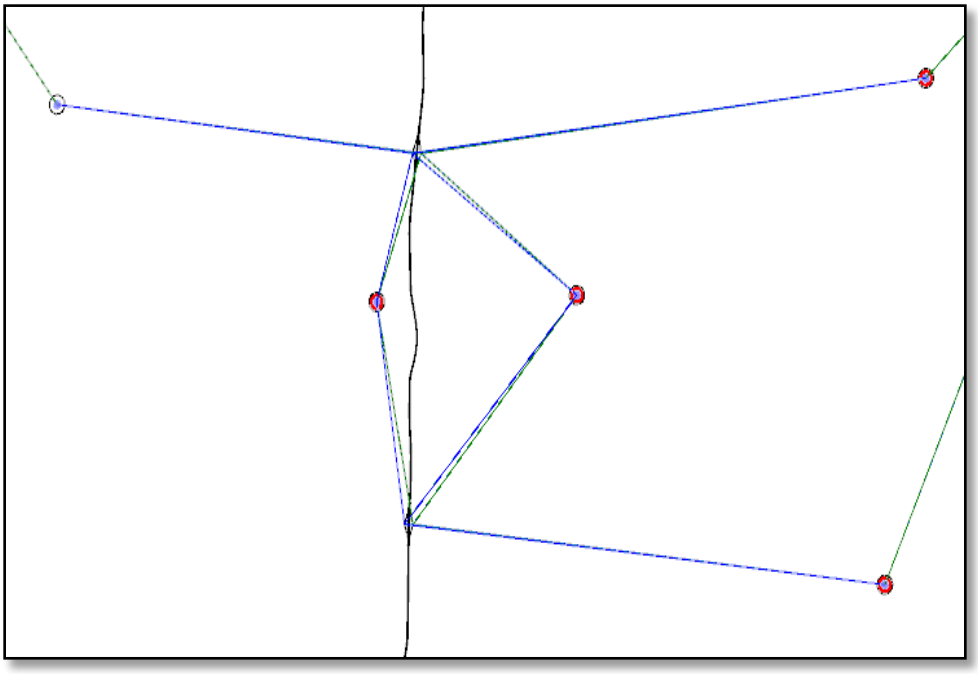

Figure 8: SuperTAZs with neighbors connected via local streets

Demand Calibration Step 3: Adjust OD Demand with observed link counts

Now that excess trips have been removed from the trip matrix, the next problem becomes the disparities in demand at individual sensor sites. Unfortunately, fixing the demand at a given site is more complicated than the previous steps.

The relationship between O-D matrix and link counts can be expressed through an assignment mapping called link use proportion (A). Basically, it represents the proportion of trips from a particular O-D pair on a specific link and is critical to the estimation problem. The representative methods for deriving O-D matrix from traffic counts includes the entropy maximization method (Van Zuylen and Willumsen, 1980), maximum likelihood method (Spiess, 1987), and the generalized least square (GLS) method (Cascetta, 1984; Bell, 1991). Due to the fact that traffic counts are usually associated with measurement errors, there may not exist an O-D matrix that can reproduce exactly these traffic counts when assigned onto the network. These methods,

which utilize the distance measures, have been proposed to select the O-D matrix with the minimum distance comparing resultant link volumes and observed traffic counts.

In this study, the constrained generalized least square (CGLS) method proposed by Bell (1991) was applied to calibrate the O-D matrix for the mesoscopic model. In fact, the proposed procedure is similar to a bi-level programming approach proposed by Yang et al (1992). Basically, the O-D matrix is adjusted according to CGLS objective, and the link use proportion (A) is updated by the mean of traffic simulation. This procedure will be iterated until the goal of calibration is met (e.g., a distance measure is less than a certain threshold). In addition to traffic counts, the prior O-D matrix can be used to assist the calibration. The preferences (or confidence) of different types of data can also be incorporated.

The Generalized Least Square (GLS) approach utilizes the information from different data sources of which accuracies are always different. The equivalent optimization of problem has the following form.

Minimize: $f(\mathbf{q}) = \omega_1 \cdot (\mathbf{q} - \bar{\mathbf{q}})^{\mathbf{T}} \cdot \mathbf{U}^{-1} \cdot (\mathbf{q} - \bar{\mathbf{q}}) + \omega_2 \cdot (\bar{\mathbf{v}} - \mathbf{A}\mathbf{q})^{\mathbf{T}} \cdot \mathbf{W}^{-1} \cdot (\bar{\mathbf{v}} - \mathbf{A}\mathbf{q})$, (1)

Subject to: $\mathbf{q} \geq 0$. (2)

The inputs to this formulation are a vector of prior O-D demand ($\bar{\mathbf{q}}$), a vector of traffic counts ($\bar{\mathbf{v}}$), variance-covariance matrices for the prior O-D demand and traffic counts (U and W respectively), and link use proportion (A). ω1 and ω2 are the preferences (weights) given to different data sources (the prior O-D matrix and traffic counts). Under the assumption that the non-negativity constraints (2) are inactive, the optimal solution to the problem can be explicitly expressed as:

$$\mathbf{q} = \left(\mathbf{U}^{-1} + \mathbf{A}^{\mathbf{T}}\mathbf{W}^{-1}\mathbf{A}\right)^{-1} \cdot \left(\mathbf{U}^{-1}\bar{\mathbf{q}} + \mathbf{A}^{\mathbf{T}}\mathbf{W}^{-1}\bar{\mathbf{v}}\right) \quad (3)$$

This expression is very useful in practice. When all information is available, the optimal (adjusted) O-D matrix can be determined using only matrix inversion and multiplication. Unfortunately, due to the assumption made above, we cannot prevent the adjusted O-D matrix from being negative. This assumption is more likely to be violated when a relatively high weight is given to one of data sources, either the prior O-D matrix or traffic counts. Bell (1991) relaxed this assumption and proposed an iterative balancing procedure to adjust the optimal solution obtained by equation (3).

Another issue is worth to consider is the prior information about trip production and trip attraction at any SuperTAZ. Without the consideration of this issue, it is possible that the estimated trips emanating from a particular zone may far exceed the number of residential units or the estimated trips terminating at a particular zone may far exceed its capacity (e.g., parking structure). This information is practically useful and leads the estimation to more reasonable ranges. This issue is also relevant to a traffic simulator. Because of the physical constraint, a traffic generator or TAZ can release only a certain number of vehicles during a certain time

period. If the estimated demand exceeds this level, there will be a lot of unreleased vehicles, which contribute nothing to the simulation results. In other words, the modeled network is under-utilized. In this study, only the constraint related to trip production (Equation 4) is incorporated to the CGLS formulation.

$$\mathbf{Bq} \le \mathbf{C}, \tag{4}$$

where B is the matrix representing the relationship between O-D pair and the origin (which O-D pair belongs to which origin), and C is the vector of capacities of TAZs. C can be determined through the simulation. By incorporating this new constraint, the Lagrangian of this formulation can be written as:

$$\Gamma(\mathbf{q}, \boldsymbol{\mu}, \boldsymbol{\lambda}) = f(\mathbf{q}) + \boldsymbol{\mu}^{\mathbf{T}}(-\mathbf{q}) + \boldsymbol{\lambda}^{\mathbf{T}}(\mathbf{Bq} - \mathbf{C}), \tag{5}$$

where μ and λ are the vectors of Lagrange multipliers for non-negativity constraint and capacity constraint for TAZ respectively. By setting the first derivative of Equation 4 with respect to q to zero, the adjusted O-D matrix can be expressed as:

$$\mathbf{q} = \left(\mathbf{U}^{-1} + \mathbf{A}^{\mathbf{T}}\mathbf{W}^{-1}\mathbf{A}\right)^{-1} \cdot \left(\mathbf{U}^{-1}\overline{\mathbf{q}} + \mathbf{A}^{\mathbf{T}}\mathbf{W}^{-1}\overline{\mathbf{v}} + \boldsymbol{\mu} - \mathbf{B}^{\mathbf{T}}\boldsymbol{\lambda}\right). \tag{6}$$

If both types of constraints are inactive, the values of Lagrange multipliers remain zero and Equation 6 collapses to equation (3), the regular GLS. If some of constraints are binding, the values of corresponding multipliers need to be adjusted by the iterative balancing technique so that those constraints are satisfied. The detailed description of iterative balancing technique can be found in Bell (1991).

As mentioned earlier, the method applied here has a similar structure to the bi-level programming approach proposed by Yang et al (1992). The adjustment process iterates between CGLS problem and traffic simulation. Firstly, the prior O-D matrix is assigned onto the network according to the logic specified in the simulation model. After that the link use proportion is determined from the simulation results and fed back to the CGLS to determine the new O-D matrix. This process is repeated until the calibration criteria (e.g., GEH-statistic ≤ 5 for more than 85 percent of observations). This adjustment procedure is summarized in Figure 9.

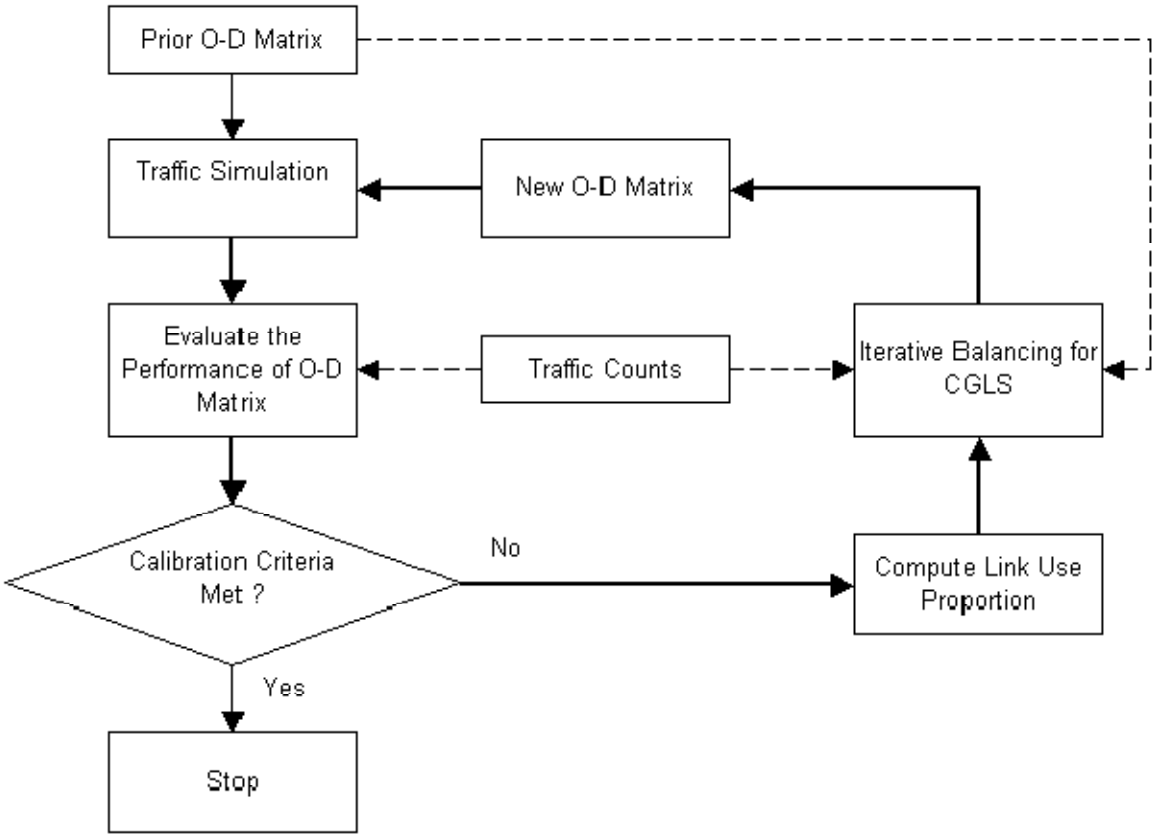

Figure 9: Procedure for OD matrix update

Demand Calibration Step 4: Manual adjustment of corridor travel to meet loop detector readings

For specific corridors, in order to make certain that the link counts from the simulation model match with those revealed from loop detector data, further manual adjustments are made using a simple set of rules and guidelines to make small, yet efficient, demand changes. A two-step process is defined below, where the steps occur sequentially:

1.) SCALE-UP/SCALE-DOWN CORRIDOR DEMAND: For this process, a common difference is defined, where the common difference is the average difference between simulated flows at sensor sites and observed flows in reality. This is done for all sensors along a given highway corridor. After determining this common difference, it is either added or subtracted from demands that normally traverse the entire corridor, as to bring all of the simulated flows closer to the observed flows.

2.) SCALE LOCAL DEMANDS AT GIVEN SITE: With simulated flows closer to observed flows, the demand differences at a given sensor site are recomputed. Additionally, the origin-destination pairs crossing that site are identified, using primarily origins and destinations nearest the sensor site, as identified by the modeler. The demand difference is proportionally added or subtracted to the given origin-destination pair, where the

proportion is defined as the demand for the given origin-destination pair divided by total demand for all origin-destination pairs in question. This is done for all sensor sites where demand differences exist. Once this is complete, the process returns to Step 1 for a different corridor.

This process will often require many iterations and attempts for any given corridor. Additionally, it may be required by the modeler working on the calibration to identify stopping criteria, such that additions and subtractions for different sites do not offset one another.

To better illustrate this procedure, a small example is used. With the corridor described in Figure 10, the following observations at the four loop detectors (blue circles) are made.

- Detector 1: Simulated Flow is 400 veh/hr BELOW observed demand
- Detector 2: Simulated Flow is 500 veh/hr BELOW observed demand
- Detector 3: Simulated Flow is 400 veh/hr BELOW observed demand
- Detector 4: Simulated Flow is 500 veh/hr BELOW observed demand

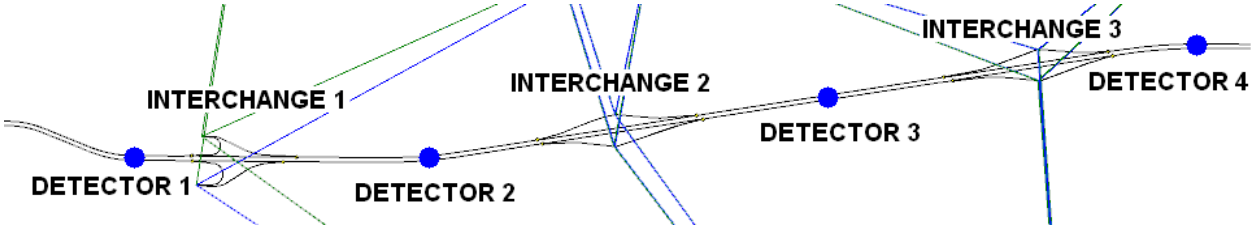

Figure 10: A corridor with observations that require trip demand matrix adjustment. Blue circles represent loop detector sites and three interchanges are present, each with their own demand

Clearly, since two detectors record simulated flows that are 400 vehicles/hour below the observed flows and two detectors record simulated flows that are 500 vehicles/hour below the observed flows, the common difference would be 450 vehicles/hour. This effectively completes the first step of the two-step process.

Applying an additional demand of 450 vehicles/hour to travel through the corridor, the following new observations are made:

- Detector 1: Simulated Flow is 50 veh/hr ABOVE observed demand
- Detector 2: Simulated Flow is 50 veh/hr BELOW observed demand
- Detector 3: Simulated Flow is 50 veh/hr ABOVE observed demand
- Detector 4: Simulated Flow is 50 veh/hr BELOW observed demand

In this simple example, the SuperTAZs (with connecting lines to respective interchanges shown in Figure 10 are unique to each interchange. Thus, the following changes to network demand need to be made to effectively solve the problem:

- Corridor Start Point → Interchange 1: Decrease demand by 50
- Interchange 1 → Interchange 2: Increase demand by 50
- Interchange 2 → Interchange 3: Decrease demand by 50
- Interchange 3 → Corridor End Point: Increase demand by 50

Between any two points, many origin-destination paths may exist. Demand along each origin-destination path must be changed to scale, based on the total demand. Among all origin-destination pairs, the amount of total change should equal the recommendation provided here.

In situations where a productive result cannot be generated (such as a recommendation of decreasing a certain demand that, in fact, does not exist in the original trip table or has a value of zero), all changes must be nullified and the calibration effort must return to Step 1 for that corridor, where a lesser common difference must be selected. If this had occurred in the example, a better selection for a common difference would have been 400 vehicles/hour.

4.2.3 Calibration Targets

Before any demand calibration can occur, it is important to define calibration targets, or acceptance thresholds, in which the simulated data can be considered "close enough" to the observed data. No uniform acceptance threshold exists to date, as levels of acceptance have largely been left to being user-defined. However, some thresholds defined by Dowling et al. (2002) have been widely used in the United States. Table 1 reflects some of the acceptance criteria proposed in that work.

Table 1: Example of acceptance criteria

Criteria & Measures	Acceptability Targets
Hourly Flows, Model vs. Observed	
Individual Link Flows	
Within 15%, for 700 vph < Flow <2700 vph	> 85% of cases
Within 100 vph, for Flow < 700 vph	> 85% of cases
Within 400 vph, for Flow > 2700 vph	> 85% of cases
Total Link Flows	
Within 5%	All Accepting Links
GEH Statistic – Individual Link Flows	
GEH < 5	> 85% of cases
GEH Statistic – Total Link Flows	
GEH < 4	All Accepting Links
Travel Times, Model vs. Observed	
Journey Times Network	
Within 15% (or one minute, if higher)	> 85% of cases
Visual Audits	
Individual Link Speeds	
Visually acceptable Speed-Flow relationship	To analyst's satisfaction
Bottlenecks	
Visually acceptable Queuing	To analyst's satisfaction

where:

$$GEH = \sqrt{\frac{(Actual - Simulated)^2}{(Actual + Simulated)/2}}$$

This work will utilize some of the general concepts of acceptability targets defined above. At a basic level, the focus of acceptability will be on three components, going from most important to

least important: observed flow vs. simulated flow at loop detectors, observed speed vs. simulated speed at loop detectors, and queue formation throughout network. With these three components, the following criteria are devised:

1.) 85 percent or more of operational loop detectors (approximately 200 in the network) must achieve a GEH statistic of less than 5 when comparing actual counts versus simulated counts. This must occur for multiple simulation runs with multiple seeds.
2.) A sufficient number (80 – 90 percent) of loop detectors observe simulated speeds that are "reasonable" relative to actual speeds. In most cases, "reasonable" would constitute a relative error of 15 percent or less, but under certain circumstances may allow for a higher threshold (e.g. both states are in free-flow and disparate because of AIMSUN parameters). This must occur for multiple simulation runs with multiple seeds.
3.) Queue formation in the network must be reasonable, based on the subjective opinion of the modeler. This criterion is considered not as relevant as the other two.

4.3 Calibration Results

4.3.1 Criteria #1: Traffic Counts

The first calibration criteria stated that 85 percent or more of the loop detectors in the network must achieve a GEH statistic of 5 or less, based on actual versus simulated flow. After utilizing the calibration procedures outlined in earlier sections, it was found that this requirement was met. This achievement occurred for multiple simulations with multiple seeds, implying that the trip matrix had been changed sufficiently to match the demand. On average, anywhere between 85 and 90 percent of the loop detectors met this requirement.

These results are revealed in Table 2 and Table 3 (the total 200 operational detectors were split into two sets to present due to space limitation on the page). In these tables, green represents detectors where the GEH statistic requirement was met and red represents detectors where the GEH statistic requirement was not met.

Table 2: GEH statistics for 1st set of loop detectors

Detector ID	Real Counts	Simulated Counts	GEH Statistic	Detector ID	Real Counts	Simulated Counts	GEH Statistic
S750	2,401	666	44.30549458	S1171	2,168	2,036	2.879105475
S813	1,033	1,448	11.78283273	S1061	4,184	3,937	3.876209092
S1393	2,231	3,119	17.16924005	S231	5,030	4,735	4.221831442
S757	1,382	1,897	12.71895757	S670	1,424	1,341	2.23226383
S207	3,051	4,182	18.80695001	S701	3,138	2,957	3.278738027
S316	3,553	4,618	16.66199502	S31	2,256	2,127	2.755617745
S1048	1,300	1,688	10.03821347	S1175	2,424	2,287	2.822792877
S1190	4,109	5,132	15.04981448	S480	4,655	4,392	3.910375391
S425	2,534	3,132	11.23512469	S738	4,022	3,796	3.61472784
S109	3,517	4,343	13.17600564	S147	4,295	4,550	3.834478082
S1164	375	305	3.796283012	S516	4,553	4,301	3.787440159
S1166	1,347	1,653	7.900886026	S369	1,338	1,264	2.0516018
S1424	2,495	3,035	10.26942653	S377	2,691	2,543	2.893076077
S572	1,960	2,359	8.586106904	S810	1,877	1,774	2.41071742
S504	2,161	2,600	8.997677592	S459	3,090	2,922	3.064183669
S710	3,113	3,695	9.975351526	S538	1,162	1,228	1.909237619
S1193	3,773	4,450	10.55816686	S1009	2,886	2,737	2.810070556
S682	4,228	4,949	10.64387821	S567	2,670	2,534	2.666154191
S897	1,247	1,458	5.737382685	S1185	3,972	4,176	3.196094819
S667	2,382	2,773	7.701537252	S495	1,577	1,657	1.989458925
S1087	3,006	3,412	7.167062224	S786	4,379	4,168	3.227680966
S81	1,320	1,485	4.405878426	S188	4,609	4,836	3.30323806
S672	784	702	3.008288237	S36	3,545	3,379	2.821269386
S944	2,573	2,304	5.44742049	S338	3,086	2,943	2.604524178
S349	851	775	2.665436371	S62	3,866	4,049	2.908979281
S1089	2,594	2,367	4.557810258	S334	2,405	2,518	2.277605608
S1111	1,407	1,540	3.464787236	S591	2,156	2,257	2.150153215
S1358	1,553	1,420	3.449603535	S347	1,034	1,082	1.475701109
S666	2,230	2,048	3.935192626	S1425	1,200	1,148	1.517641854
S1115	2,267	2,468	4.130960702	S451	3,777	3,615	2.664704365
S976	1,161	1,261	2.873610676	S1412	2,593	2,709	2.252958154
S226	3,716	3,427	4.835846595	S595	2,412	2,519	2.154920607
S916	2,304	2,495	3.899177359	S168	4,240	4,067	2.684349103
S394	2,504	2,708	3.996160859	S800	4,861	5,062	2.853576761
S722	2,114	1,955	3.525074316	S921	2,245	2,156	1.897270789
S343	3,101	2,880	4.041293295	S504	2,161	2,250	1.895118956
S769	2,911	3,130	3.984783173	S299	4,568	4,756	2.753415258
S730	2,467	2,652	3.656740666	S684	4,514	4,336	2.67585986
S1074	3,041	2,829	3.913197867	S1042	2,677	2,573	2.029872152
S584	1,362	1,462	2.661231477	S1169	2,241	2,331	1.882367415
S988	1,715	1,598	2.874684198	S1112	1,352	1,300	1.428011095
S1357	1,643	1,763	2.90786287	S216	2,138	2,223	1.820291245
S42	3,004	3,223	3.924819421	S430	3,050	3,171	2.169553018
S956	2,486	2,319	3.407099156	S1160	1,368	1,316	1.419472835
S1063	2,882	2,694	3.56050389	S1165	813	845	1.111405939
S1360	3,721	3,980	4.173891931	S215	3,755	3,618	2.256386268
S233	4,269	3,996	4.246745311	S1053	1,560	1,504	1.430733165
S1010	4,700	5,021	4.604310026	S1076	3,583	3,716	2.201582462
S654	2,997	2,813	3.413852514	S677	2,107	2,185	1.683758278
S781	2,891	3,079	3.441007994	S208	2,901	2,798	1.929536037

Table 3: GEH statistics for 2nd set of loop detectors

Detector ID	Real Counts	Simulated Counts	GEH Statistic	Detector ID	Real Counts	Simulated Counts	GEH Statistic
S665	2,364	2,451	1.773111737	S255	5,297	5,217	1.10336956
S1405	3,099	2,989	1.993748442	S836	3,035	3,081	0.831838642
S622	4,159	4,012	2.299824665	S679	2,713	2,754	0.784195449
S1078	2,978	3,084	1.925364221	S276	2,801	2,760	0.777539403
S439	3,805	3,939	2.153461561	S225	4,690	4,622	0.996557649
S323	2,944	3,047	1.881926088	S1085	3,310	3,358	0.831301262
S641	6,037	6,248	2.692215825	S478	4,506	4,442	0.956823832
S330	1,749	1,690	1.422823146	S617	2,959	2,918	0.756346862
S511	3,475	3,594	2.00162616	S356	3,206	3,248	0.739349541
S797	1,422	1,375	1.256801304	S928	1,374	1,357	0.460047918
S827	3,556	3,671	1.913082993	S527	2,606	2,574	0.628781994
S21	3,554	3,443	1.876644627	S463	1,612	1,632	0.496597548
S241	1,351	1,309	1.151657844	S151	4,536	4,592	0.828924945
S887	3,498	3,394	1.77164092	S785	6,290	6,367	0.967921937
S86	4,397	4,529	1.975879647	S1426	760	751	0.327435132
S792	4,563	4,434	1.923339044	S606	2,389	2,416	0.550848367
S553	5,650	5,496	2.062890611	S301	1,797	1,815	0.423558725
S872	2,427	2,361	1.348906547	S409	5,267	5,216	0.70443736
S679	2,713	2,641	1.391580424	S1158	1,525	1,511	0.359328902
S183	3,968	3,863	1.678014406	S444	2,954	2,981	0.495642342
S148	5,167	5,031	1.904567646	S382	4,458	4,418	0.600435474
S778	5,727	5,579	1.968440186	S1069	4,313	4,276	0.564605911
S4	4,853	4,980	1.811238743	S602	1,548	1,537	0.280078711
S692	5,069	5,201	1.842059725	S1359	3,633	3,659	0.430591067
S848	2,693	2,763	1.340219267	S683	4,308	4,336	0.425907855
S910	3,991	3,890	1.608961706	S855	3,108	3,128	0.358172254
S200	4,598	4,485	1.676790421	S903	1,443	1,452	0.236555594
S377	2,691	2,626	1.26065144	S353	3,580	3,559	0.351492127
S878	3,423	3,343	1.375431569	S1418	2,379	2,366	0.26689488
S232	3,958	3,867	1.454836596	S1058	3,066	3,081	0.27056689
S829	3,819	3,733	1.399530793	S1178	2,286	2,297	0.229790862
S962	3,073	3,004	1.251755391	S761	2,588	2,576	0.236158253
S267	1,817	1,779	0.896166598	S414	5,281	5,257	0.330633719
S327	2,338	2,290	0.9978369	S1163	927	923	0.13151919
S1199	2,587	2,641	1.056187366	S1196	3,095	3,108	0.233430424
S1116	3,503	3,576	1.227020735	S657	2,973	2,962	0.201928362
S888	1,839	1,877	0.881577996	S240	6,237	6,214	0.291501449
S579	2,178	2,223	0.959294219	S1204	2,596	2,587	0.176793748
S980	1,537	1,568	0.786766554	S746	3,772	3,784	0.19523167
S234	3,573	3,645	1.198502807	S1154	1,578	1,573	0.125968164
S46	3,417	3,482	1.10671369	S419	4,369	4,381	0.181422947
S775	5,639	5,536	1.377934128	S613	3,701	3,711	0.164265853
S195	5,078	5,172	1.313048956	S1151	1,907	1,902	0.114572269
S788	5,781	5,677	1.374022765	S313	3,423	3,429	0.102507955
S776	4,470	4,551	1.206070446	S398	5,783	5,774	0.118395433
S271	3,648	3,584	1.064304168	S426	2,631	2,627	0.07801259
S387	5,817	5,719	1.2903676	S554	5,466	5,461	0.067644818
S264	1,913	1,945	0.728591104	S695	4,665	4,662	0.043930411
S1399	2,762	2,808	0.871656217	S952	1,585	1,584	0.025121981
S970	2,354	2,316	0.786393933	S294	4,770	4,772	0.028955115

4.3.2 Criteria #2: Speeds

The second calibration criteria stated that a sufficient number of loop detectors must report simulated speeds within 15 percent of the observed or have a “reasonable” explanation for failing to meet this criterion. Focusing on speed alone, it was found that roughly 60 percent of the loop detectors met the requirement of coming within 15 percent of the observed speed. Additionally, 25 percent of the total did not meet the requirement, but had a unique circumstance. In this situation, it was observed that the simulated velocity at the detector was the maximum velocity, suggesting a free-flow state (e.g. 60 miles per hour). In the real-world, the actual velocity reported by the detector was significantly higher (e.g. 80 miles per hour). It can be inferred that this actual velocity is a free-flow state as well and the only reason for the disparity was because of the 60 mile-per-hour maximum speed requirement defined in AIMSUN. Thus, these situations could be included as acceptable results, bringing the total to 85 percent of all detectors meeting the requirement.

These results are revealed in Table 4 and Table 5. In these tables, green represents detectors where the relative error requirement was met for speed, yellow represents detectors where the relative error requirement was met for speed, in terms of both being at a free-flow state, and red represents detectors where the GEH statistic requirement was not met.

Table 4: Relative error for speed of 1st set of loop detectors

Detector ID	Real Speed (km/hr)	Simulated Speed (km/hr)	Relative Error	Detector ID	Real Speed (km/hr)	Simulated Speed (km/hr)	Relative Error
S750	71.6508416	78.6	9.70%	S1171	119.5063104	96.51	19.24%
S813	108.7845216	97.47	10.40%	S1061	119.465184	91.18	23.68%
S1393	105.88616	97.37	8.04%	S231	123.010736	94.28	23.36%
S757	105.955088	82.63	22.01%	S670	100.7922784	98.37	2.40%
S207	120.180496	95.39	20.63%	S701	52.3866768	93.07	77.66%
S316	84.1078496	90.94	8.12%	S31	103.5447264	96.79	6.52%
S1048	108.67072	96.31	11.37%	S1175	113.673232	93.34	17.89%
S1190	112.282816	92.62	17.51%	S480	110.157184	96.01	12.84%
S425	101.7181216	100.63	1.07%	S738	80.408576	91.7	14.04%
S109	79.1262448	95.6	20.82%	S147	105.12408	96.52	8.18%
S1164	124.318848	92.17	25.86%	S516	119.90872	92.52	22.84%
S1166	119.898576	99.09	17.36%	S369	94.973736	96.31	1.41%
S1424	39.853216	93.35	134.23%	S377	102.962128	97.14	5.65%
S572	95.9841792	92.78	3.34%	S810	105.37024	96.92	8.02%
S504	99.082704	93.55	5.58%	S459	101.437168	91.31	9.98%
S710	108.684736	99.7	8.27%	S538	104.339984	95.48	8.49%
S1193	116.7449216	92.06	21.14%	S1009	112.652552	100.38	10.89%
S682	94.5156864	93.92	0.63%	S567	25.952024	96.19	270.65%
S897	117.8003904	103.6	12.05%	S1185	110.3913216	90.83	17.72%
S667	115.5626464	99.73	13.70%	S495	79.3052736	96.84	22.11%
S1087	93.6893008	91.61	2.22%	S786	36.8114896	92.82	152.15%
S81	118.275008	101.87	13.87%	S188	111.848192	96.43	13.78%
S672	123.23264	99.48	19.27%	S36	108.532688	95.4	12.10%
S944	110.339368	97.44	11.69%	S338	101.83324	94.42	7.28%
S349	115.791792	103.52	10.60%	S62	108.452896	93.81	13.50%
S1089	118.853952	93.11	21.66%	S334	31.1601984	94.01	201.70%
S1111	135.69576	94.32	30.49%	S591	105.5158816	94.66	10.29%
S1358	117.751136	91.16	22.58%	S347	103.304456	95.65	7.41%
S666	111.2970944	98.81	11.22%	S1425	96.093392	98.79	2.81%
S1115	138.558784	97.53	29.61%	S451	94.7232544	92.49	2.36%
S976	111.591472	102.12	8.49%	S1412	111.700496	93.63	16.18%
S226	119.418528	92.36	22.66%	S595	103.9999264	95.27	8.39%
S916	117.998944	94.64	19.80%	S168	108.198768	94.27	12.87%
S394	108.73504	94.46	13.13%	S800	97.6117008	94.21	3.48%
S722	107.904248	99.86	7.45%	S921	109.484632	101.31	7.47%
S343	102.3542304	92.75	9.38%	S504	99.082704	93.55	5.58%
S769	104.900592	93.22	11.13%	S299	121.092544	93.77	22.56%
S730	93.6687136	95.07	1.50%	S684	110.703088	95.56	13.68%
S1074	56.86888	95.38	67.72%	S1042	111.62024	94.37	15.45%
S584	69.925744	99.15	41.79%	S1169	127.601168	97.28	23.76%
S988	114.933968	98.59	14.22%	S1112	133.000232	92.7	30.30%
S1357	125.968896	92.83	26.31%	S216	119.721856	94.41	21.14%
S42	57.979216	95.33	64.42%	S430	105.282464	94.1	10.62%
S956	110.8916	97.25	12.30%	S1160	118.0548704	102.12	13.50%
S1063	108.811056	92.17	15.29%	S1165	122.101728	90.84	25.60%
S1360	119.804456	94.08	21.47%	S215	132.286736	94.96	28.22%
S233	120.02616	96.83	19.33%	S1053	128.58988	93.12	27.58%
S1010	111.931856	97.74	12.68%	S1076	88.298496	95.29	7.92%
S654	101.7579104	95.94	5.72%	S677	159.717688	93.48	41.47%
S781	97.7680544	96.28	1.52%	S208	118.224912	95.69	19.06%

Table 5: Relative error for speed of 2nd set of loop detectors

Detector ID	Real Speed (km/hr)	Simulated Speed (km/hr)	Relative Error	Detector ID	Real Speed (km/hr)	Simulated Speed (km/hr)	Relative Error
S665	112.20824	99.39	11.42%	S255	106.292144	92.9	12.60%
S1405	104.6293824	94.54	9.64%	S836	96.2376896	80.06	16.81%
S622	96.7764704	93.89	2.98%	S679	77.82272	94.03	20.83%
S1078	100.9423648	94.64	6.24%	S276	107.10448	94.7	11.58%
S439	102.49864	90.75	11.46%	S225	120.546336	95.59	20.70%
S323	76.629856	94.99	23.96%	S1085	107.793408	92.13	14.53%
S641	81.1710752	90.89	11.97%	S478	89.8391472	95.64	6.46%
S330	94.182992	95.25	1.13%	S617	91.6084832	96.15	4.96%
S511	119.9397824	94.23	21.44%	S356	87.6380928	93.86	7.10%
S797	65.150752	101.34	55.55%	S928	105.128288	101.75	3.21%
S827	118.3111936	94.36	20.24%	S527	105.542016	92.19	12.65%
S21	90.463968	94.31	4.25%	S463	99.3776	89.87	9.57%
S241	104.718768	95.42	8.88%	S151	58.9850464	93.29	58.16%
S887	114.706784	98.74	13.92%	S785	63.1843744	91.87	45.40%
S86	89.181	95.31	6.87%	S1426	99.131552	92.2	6.99%
S792	44.1998112	91.72	107.51%	S606	102.31408	89.28	12.74%
S553	88.936976	91.39	2.76%	S301	94.0955936	98.1	4.26%
S872	118.057616	99.08	16.07%	S409	78.4364864	90.27	15.09%
S679	77.82272	94.03	20.83%	S1158	111.953784	93.47	16.51%
S183	28.9068304	92.59	220.30%	S444	107.742848	99.53	7.62%
S148	45.9615424	93.35	103.10%	S382	104.432896	92.65	11.28%
S778	103.2304	93.58	9.35%	S1069	48.5457344	92.84	91.24%
S4	103.924	93.58	9.95%	S602	97.7198784	94.2	3.60%
S692	114.593232	92.22	19.52%	S1359	105.035536	98.63	6.10%
S848	104.608528	79.99	23.53%	S683	111.967024	95.31	14.88%
S910	115.720624	97.29	15.93%	S855	100.7230048	92.23	8.43%
S200	102.0414608	95.64	6.27%	S903	84.935584	96.78	13.95%
S377	102.9621	97.14	5.65%	S353	67.6209344	94.35	39.53%
S878	121.752176	100.54	17.42%	S1418	113.05496	93.25	17.52%
S232	119.52352	92.85	22.32%	S1058	122.515264	93.66	23.55%
S829	95.290592	93.29	2.10%	S1178	79.821832	93.17	16.72%
S962	109.3912224	95.44	12.75%	S761	99.439216	94.24	5.23%
S267	101.5210992	95.32	6.11%	S414	97.7252384	93.47	4.35%
S327	90.4507936	93.3	3.15%	S1163	127.232776	97.91	23.05%
S1199	115.501344	93.71	18.87%	S1196	117.966848	92.14	21.89%
S1116	124.114392	94.51	23.85%	S657	102.604336	93.43	8.94%
S888	108.3250496	99.71	7.95%	S240	99.331128	94.92	4.44%
S579	18.2012208	94.48	419.09%	S1204	116.353504	92.43	20.56%
S980	115.427312	99.23	14.03%	S746	64.425648	92.82	44.07%
S234	121.758816	96.71	20.57%	S1154	99.496752	96.55	2.96%
S46	105.018112	94.81	9.72%	S419	106.563504	95.41	10.47%
S775	93.127376	91.5	1.75%	S613	101.384368	93.02	8.25%
S195	81.867488	94.19	15.05%	S1151	100.8497008	97.9	2.92%
S788	44.4007408	92.91	109.25%	S313	95.54	95.54	0.00%
S776	99.838208	94.62	5.23%	S398	89.150128	91.98	3.17%
S271	109.93152	94.1	14.40%	S426	106.415992	98.52	7.42%
S387	93.574304	91.15	2.59%	S554	92.4455936	92.1	0.37%
S264	117.4836544	98.92	15.80%	S695	105.61432	95.5	9.58%
S1399	116.604968	95.29	18.28%	S952	112.216672	98.9	11.87%
S970	105.636112	99.16	6.13%	S294	115.9524	96.87	16.46%

4.3.3 Criteria #3: Queue Formation

From subjective observation, the resultant queues appear (visually) to be forming in areas where queues form in reality. Thus, the requirement is met.

5 Applications of Mesoscopic Simulation Model

5.1 Network Performance Changes after the I-35W Bridge Collapse/Reopening

After the I-35W Bridge collapse, the changes in the network infrastructure forced some drivers to change their routes and, thus, change the equilibrium state. With the calibrated mesoscopic traffic simulation model, the long-term traffic patterns following the I-35W Bridge collapse and reopening can be simulated. Here, three specific networks are designed to represent the three networks present: before collapse (July 2007), after collapse (October 2007), and after reopening (November 2008). We note that the bridge collapsed on Aug. 1, 2007 and it was reopened on Sept. 18, 2008. Performance measures were calculated through AIMSUN for each of the networks. The results for these performance measures are listed below in Table 6.

Table 6: Network-level performance measures before and after bridge collapse

	Jul-07	Oct-07	Nov-08
Delay (secs/km)	7.0086	7.11019	6.99795
Density (veh/km)	10.51	10.55	10.48
Flow (veh/hr)	352,220	352,031	352,169
Speed (km/hr)	81.191	80.996	81.201
Travel Time (secs/km)	48.12	48.31	48.11

As shown, delay, density, and travel time went up following the bridge collapse. Similarly, these three performance measures went down following reopening. It is important to note that, since the network following reopening had more capacity than the one before collapse (e.g. the "extra" lane on I-94 remained after reopening, the bridge had one extra lane), performance measures after reopening are "better" than before collapse. This type of data is very helpful for studying cost-benefit analysis of reopening schedules and other construction activities.

5.2 Perceived Cost Model Development

Another research topic that is worth investigating is how drivers are psychologically influenced by the tragedy surrounding the bridge collapse. Using mesoscopic traffic simulation in AIMSUN, this investigation can be conducted.

Despite the tragedy of the bridge collapse, the vast majority of loop detector infrastructure around the Twin Cities remained fully operational. Using loop detectors on all Twin Cities on-ramps to capture traffic counts, the total traffic demand to the freeway was assessed on a daily basis during a three-hour period in the AM Peak. Data was collected between July 23rd, 2007, and August 31st, 2007, to determine if the bridge collapse caused a significant change in freeway demand. These daily total counts are provided in Figure 11.

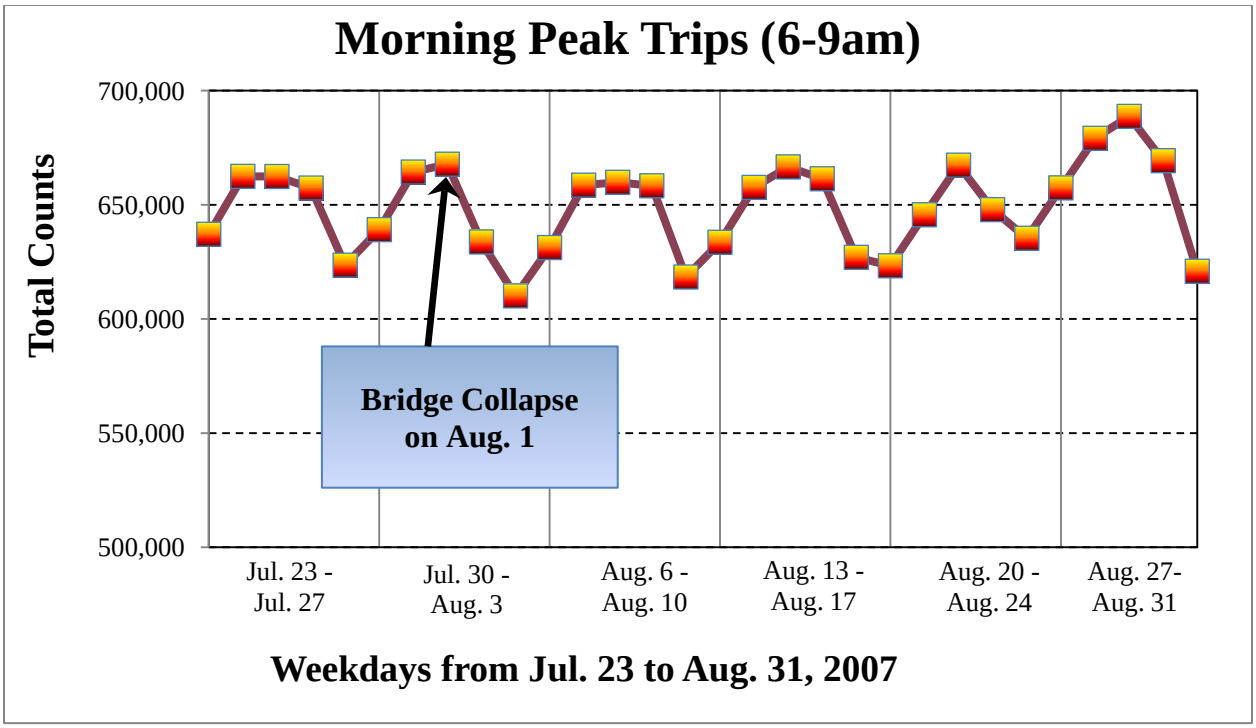

Figure 11: Daily trips entering the Twin Cities freeway network via on-ramps

As revealed by the on-ramp data, freeway traffic demand in the days and weeks following the bridge collapse does not experience any drastic changes, fluctuating within the bounds of weekly variation. The lone exception is on Thursday, August 2nd, where a noticeable decrease occurs when compared to other Thursdays, but otherwise demand remains consistent with previous weeks. This shows that the bridge collapse did not influence freeway demand during the AM Peak on the system as a whole. Given this, the next question is how, if at all, the bridge collapse influenced traffic within the network.

Several zonal regions will be defined around the bridge collapse site. These zonal regions do not necessarily have a Euclidean radius, as such a radius would likely encompass biased infrastructure features (e.g. accounting for a major interchange on one side of the zone, but not the other). Instead, the boundaries of these zones are defined by cordon lines drawn in a manner to uniformly capture similar network topology. For example, a cordon may be drawn around the bridge site to entirely include the T.H. 280 alternative route, as to study I-35W corridor traffic. These cordon lines serve as counting points, where all traffic entering the cordon is tallied and aggregated over the analysis period.

Five cordons are proposed, shown in Figure 12. The network topologic features intended to be captured are discussed in Table 7. For reference, Cordon 1 refers to the smallest cordoned area near bridge while Cordon 5 refers to the largest cordoned area around the metropolitan area.

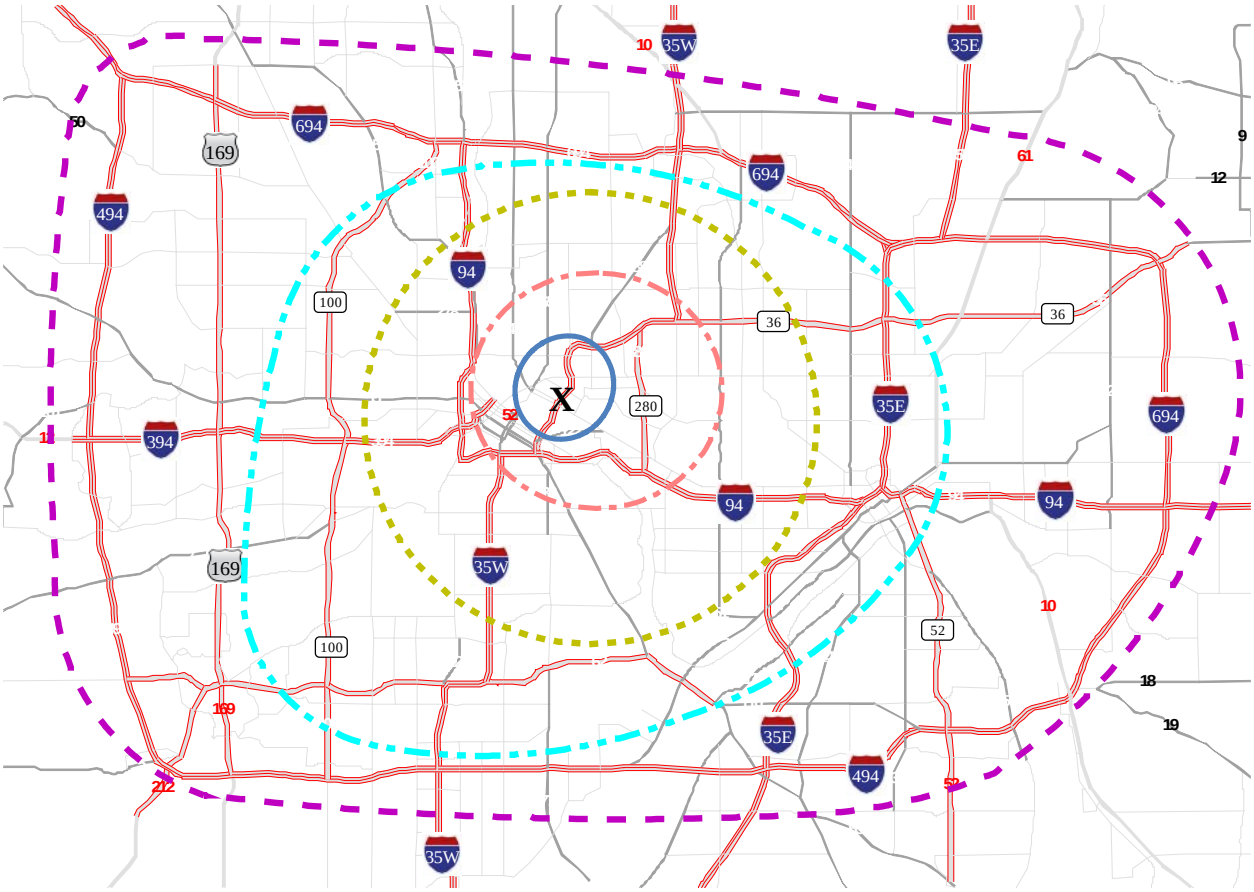

Figure 12: Five cordon circles around the Twin Cities

Table 7: Network topologic features of cordoned areas

Cordon Number	Region within Cordon	Network Topology Features	Approximated Cordon Radius (miles)
1	Immediate Area of I-35W Bridge	No alternative routes within cordon. No freeway connectivity within cordon. Traffic approaching bridge is forced to exit.	0.5
2	I-35W/I-94 Corridor Interchange	Includes I-94 corridor and I-35W (using T.H. 280 detour) corridor. No freeway-based alternative routes within cordon.	2.5
3	City of Minneapolis and Minneapolis Central Business District	Includes all routes bound for Minneapolis. Some freeway-based alternative routes.	5.5
4	Minneapolis and St. Paul Central Business District	Includes all routes heading toward central business district in either city. Many freeway-based alternative routes.	8.5
5	Twin Cities Metropolitan Area	Includes all routes approaching the I-494/I-694 beltway. Many freeway-based alternative routes.	15

The aggregated counts entering these cordons will be analyzed for each non-holiday weekday between Monday, July 9th, 2007, and Friday, November 16th, 2007. The period in which traffic is counted will be during the AM peak period as the vast majority of trips in this time period are usually inflexible ones, such as journeys to work or school. To avoid issues of skewed data due to peak spreading, the AM peak period is designated between 6 a.m. and 10 a.m. local time. Thus, the aggregated total for each day consists of four hours of traffic counts.

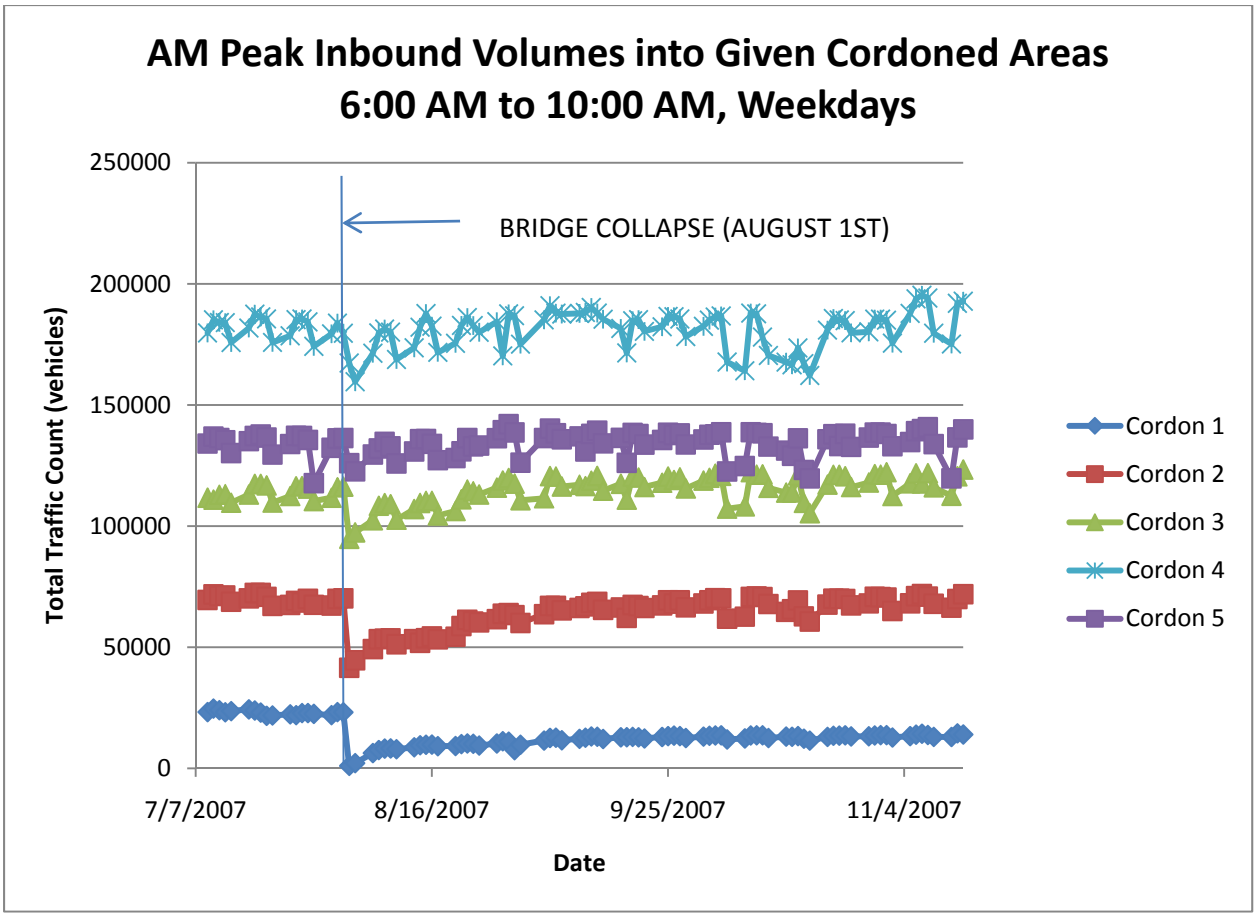

Figure 13: Total traffic counts for each cordon circle

Figure 13 illustrates the evolution of daily four-hour traffic counts over the analysis time frame. Prior to the bridge collapse, traffic counts are mostly stable for all five cordons. However, after the collapse, some of these counts dramatically change. The traffic demand at Cordon 1 drops to nearly zero while demand at Cordon 2 and Cordon 3 decreases as well. In the weeks following the collapse, the demand at these three cordons undergoes a recovery process to a certain stabilizing point in the long term. These demand changes are not observed at Cordon 4 or Cordon 5, where total demand stays relatively stable across the entire time period.

Taking a closer look at the cordons, it is seen that these dramatic demand decreases, or "shocks," diminish in intensity as alternatives become available, generally corresponding to an increase in distance from the bridge. Between pre-collapse demands and demands observed a week following the collapse, Cordon 1, Cordon 2, and Cordon 3 experience shocks of 67 percent, 25 percent, and 6.5 percent, respectively, while Cordon 4 and Cordon 5 experience no noticeable shocks. Similarly, aside from Cordon 1, the recovery rate to pre-collapse demand is faster when more alternatives are available, as Cordon 2 and Cordon 3 recover by September 28th and August 24th, respectively, and Cordon 4 and Cordon 5 recover seemingly instantaneously. Cordon 1 can be considered a unique case as, given a severed corridor and no alternative routes within the cordon, the long-term post-collapse demand is more than 40 percent lower than pre-collapse demand. Thus, recovery to this substandard demand occurs in a relatively short time, achieving

stability on around August 24th. Stability, for this work, was considered present for a given cordon when week-by-week demands vary only by a few percentage points.

When analyzing 2005 and 2006 data for the same time period, these shocks and recoveries are not observed, revealing that they are a consequence of the bridge collapse. Moreover, as shown by the daily demand for the freeway in Figure 11, the magnitude of AM commuters over this time period remains largely unchanged, suggesting that the decreases in demand corresponds with a desire of avoidance for these cordons. This is particularly interesting because this avoidance phenomenon results in spare capacity within the cordoned areas. Traditional route choice models would favor these underutilized areas, but evidence in Figure 13 reveals such favoring occurs after an extended period of time. Thus, travelers' perceived travel cost or risk, is likely greater than the actual travel cost, which discourage usage of these roads close to the bridge.

The question becomes how these perceived costs would appear in the network to create the avoidance phenomenon? Given the driver reluctance to enter a cordon, it is easily imagined that these costs are a perceived penalty, or risk, associated with entering a zone. With the difference in alternatives between cordons, different costs could be inferred at each zone.

To create the avoidance phenomenon, a perceived cost is added to the route travel cost for routes that use the avoided cordoned areas. Since it is applicable to only those routes, it can be inferred that the perceived cost is a fee for entering the cordoned area, similar to a cordon toll. Cordon tolling is a technique used in practice and is known as a second-best tolling scheme, where only certain roads in a given area (e.g. roads along a cordon line) receive tolls while others may not. This contrasts a first-best tolling scheme, where all roads within a given area have some form of toll. Cordon pricing has been studied in the past and has been deployed in cities such as London, Singapore, and Stockholm.

Traditionally, a cordon-based tolling scheme works by charging users a monetary fee to achieve a traffic demand into the cordoned area. For this work, the fee will be a perceived cost instead of a monetary cost that will achieve a certain traffic demand. To find these costs, the calibrated mesoscopic simulation model of the Twin Cities network will be used to find traffic demands entering the cordons, using the AIMSUN traffic simulation software.

Using the mid-July 2007 calibrated traffic demands, the Twin Cities network was simulated without the I-35W Bridge or cordon tolls. The traffic demand crossing the cordons was found to match the long-term traffic demand observed in reality, suggesting that the absence of the perceived cordon tolls results in the long-term stable pattern. In the short term, however, such perceived costs would be needed to discourage use. A brute-force search procedure was used to find the additional cordon cost required to generate a given cordon entry demand. This was done on a week-by-week basis, using averaged demands over all non-holiday weekdays for that week, and by only instituting costs on Cordon 1, Cordon 2, and Cordon 3, since these are the only three that experience the avoidance phenomenon and Cordon 4 and Cordon 5 are already experiencing an accurate simulated demand. The resulting costs for each week are shown in Figure 14.

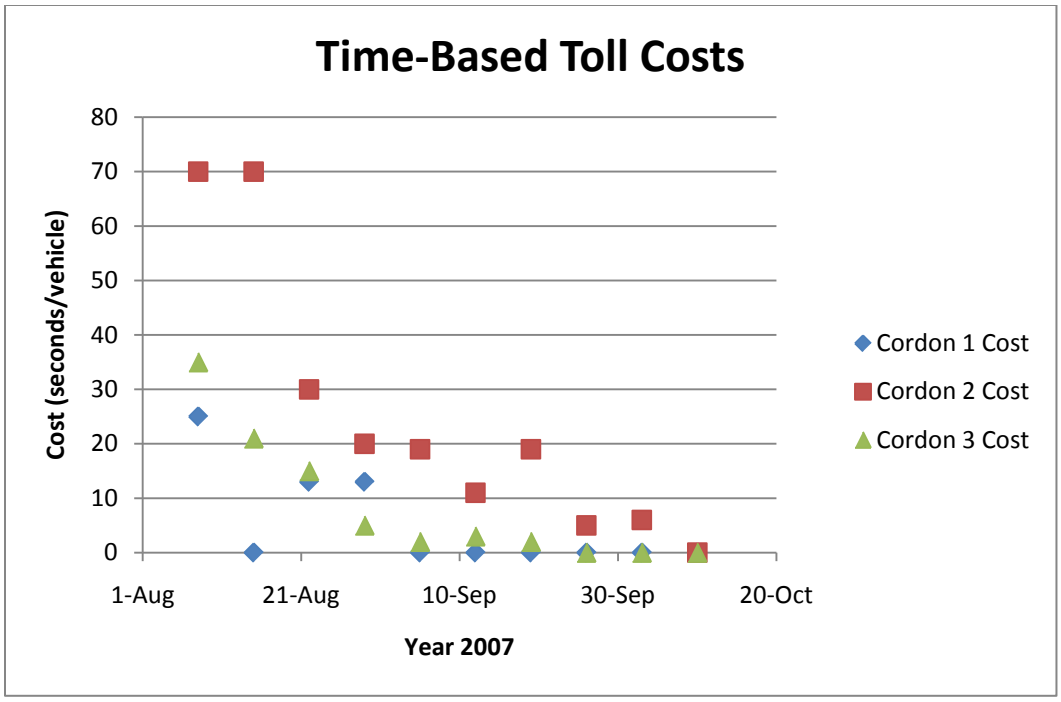

Figure 14: Time-based toll costs, as computed in the Twin Cities model

Initially, the perceived cordon costs are all relatively high, suggesting a strong influence immediately after the bridge collapse. However, with each passing week, these costs decrease at a diminishing rate of return. At the tenth week and beyond, the costs all approach zero, which results in the stabalized pattern witnessed in the long term. Given the characteristics of this data, the trend best fits an exponential decay function, where the decreasing rate of the curve is proportional to its functional value. This is verified by curve-fitting software as the preferred function for all three cordons.

The solution to this exponential decay function would be the perceived cost, C, for a given week, t. This function is composed of two coefficients, which include the initial cost, C_0, and a decay constant, λ. The function can be formulated in Equation 1.

$$C = C_0 e^{-\lambda t} \tag{1}$$

Using optimization software, the coefficients are estimated for all three cordons. The recommended values are shown in Table 8.

Table 8: Coefficient values for cordon circles

	Initial Cost (seconds/vehicle)	Decay Constant (1/week)	R-Squared	Correlation Coef.
Cordon 1	35.94	0.53435	0.604	0.777
Cordon 2	107.75	0.34942	0.916	0.957
Cordon 3	60.767	0.53741	0.986	0.993

Overall, the proposed function fits the data. Cordon 1 is the exception, as data to be shown later reflects that the simulated result is significantly below the observed result, resulting in a lower R-Squared value. However, given the proximity of Cordon 1 and the construction activities occurring near the site following the collapse, the disparity is likely due to extra trips by construction vehicles that normally are not part of AM peak trips and, thus, not reflected in the calibrated O/D table. For Cordon 2 and Cordon 3, though, the curves fit very accurately. Using the proposed coefficients, Figure 15 reflects the appearance of the perceived cost curves.

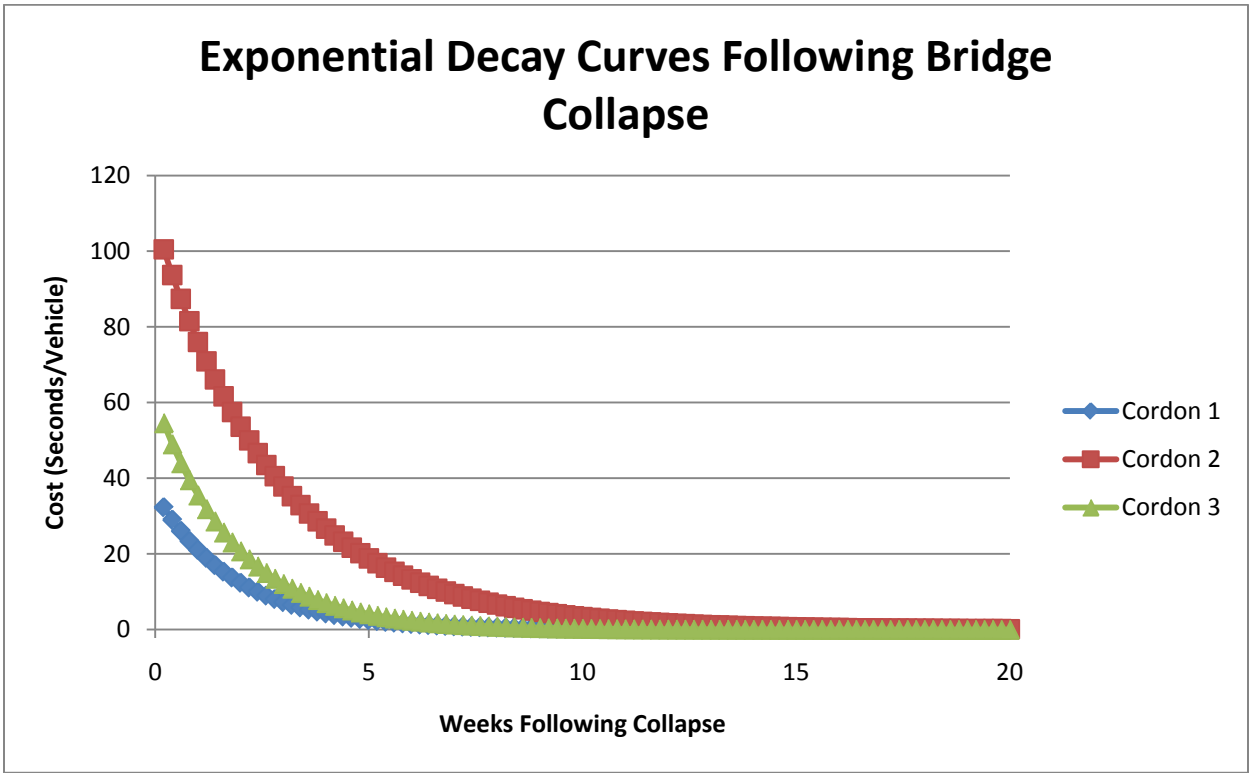

Figure 15: Exponential decay curves for given cordons

While fortunate to rarely occur, the absence of other large-scale, long-term network disruption scenarios due to an unexpected tragedy makes it impossible to model with any certainty the initial costs and decay constant for the cordons. This is left for future research, but some initial observations can be made. Ignoring Cordon 1 for now, it can be seen that the initial cost coefficient decreases as distance from the bridge and the number of alternatives increases. Cordon 2 has the fewest alternative routes and has a high initial cost, while Cordon 3 has more alternative routes and a lower initial cost. Cordon 4 and Cordon 5 have initial costs of zero, given the absence of perceived costs, and are the farthest and have the most alternative routes. The

same observation can be made for the decay constant, which increases as distance from the bridge and number of alternative routes increases. Cordon 2, which is closest and has fewest alternative routes, has a very low decay constant while Cordon 3 has a higher decay constant.

To understand the differences of Cordon 1 from these trends, it is important to recall that no connecting freeways and no freeway-based alternative routes exist within this cordon. Thus, any drivers that are intent on using the I-35W corridor must use the detour route outside of Cordon 1, resulting in a natural decrease in long-term demand. This reduced demand could easily explain the disparity of the coefficients for Cordon 1 with respect to the trends of other cordons. Unfortunately, it prevents a good correlation to determine the initial cost and decay constant from being established.

The actual estimation of these coefficients may, in fact, require more elements than simply alternative routes and relative location to the bridge. Such elements might include available system capacity within the cordon, local driver habits, costs of cordons that are within a given cordon, or psychological significance of the disruption in question. Additionally, initial costs and decay constants may change given the total number of cordons, their proximity to one another, or the traffic management along the borders. For now, the cordons will be kept constant throughout this work, leaving the exploration of different cordon sizes, numbers, and locations to future research.

How well does the proposed perceive cost model reproduce the traffic flows observed following the I-35W Bridge collapse? Using the AIMSUN mesoscopic simulation software for the Twin Cities network, analysis is conducted on a week-by-week basis to determine if vehicular flows entering the designated cordons, where the cordons are assessed a perceived cost for that week as determined by the model, match the observed counts in reality. Relative accuracy is determined using the GEH statistic, used in Dowling et al. (2002), for a cordon, where a GEH statistic of less than 5 is considered acceptable for calibration standards. Ten weeks following the bridge collapse were simulated using the perceived cordon cost model. The resulting statistics are reported in Table 9.

Table 9: Simulated and observed flows on a week-by-week basis following I-35W bridge collapse, along with the corresponding GEH statistic

	Cordon 1			Cordon 2			Cordon 3		
Week	Real Flow	Simulated Flow	GEH	Real Flow	Simulated Flow	GEH	Real Flow	Simulated Flow	GEH
1	1906	1970	1.45	13044	11945	9.83	26596	26288	1.89
2	2347	2306	0.85	13325	13821	4.26	27083	27250	1.01
3	2451	2452	0.02	14760	14578	1.5	27987	28475	2.9
4	2485	2484	0.02	15637	14949	5.56	29137	29072	0.38
5	3018	2616	7.57	16435	16392	0.33	29305	29219	0.5
6	3156	2624	9.9	16775	16695	0.61	29385	29320	0.38
7	3192	2640	10.22	16456	16915	3.55	29254	29426	1
8	3278	2644	11.65	17021	16942	0.6	29652	29463	1.1
9	3280	2651	11.55	16982	17064	0.63	29414	29526	0.65
10	3283	2649	11.64	17146	17105	0.31	29443	29555	0.65

For Cordon 1, the GEH statistic meets the requirement for the first four weeks. Following that fourth week, the threshold is violated, but this is likely due to the increased construction activities following the bridge collapse not being accounted for in the calibrated demand table in AIMSUN. For Cordon 2, eight of the ten weeks met the GEH statistic requirement, while the other two weeks come within a relative error of ten percent. While not perfect, this result is still favorable. For Cordon 3, all ten weeks meet the GEH statistic requirement. Given the low relative errors and satisfactory GEH statistics for Cordon 2 and Cordon 3, it is reasonable to say that this model has accurately proposed perceived costs that reproduce traffic demand along the cordons.

This exploration offers a mere glimpse into the research opportunities made available with the mesoscopic traffic simulation model. Many other ideas may be proposed that could use this software to generate needed evidence.

6 Conclusions

To date, large-scale microscopic traffic simulations have been difficult due to the lack of fine detail or the time requirement needed to calibrate such details. In this project, a large-scale mesoscopic traffic simulation model was developed for the Twin Cities network, using the mesoscopic traffic simulation tools available in AIMSUN 6 software. This model includes freeways, major arterials, and other roads of user-defined importance. After given an approximately origin-destination table from a planning model, the demands were calibrated to meet a set of desired practice-oriented calibration targets. These calibrated values deem to be representative of conditions present in late July 2007.

We further applied the calibrated mesoscopic simulation model to replicate the traffic dynamics after unexpected network disruption. This study proposed a simple concept to explain traffic dynamics on the Twin Cities network following the collapse of the I-35W Bridge. After witnessing an avoidance phenomenon in which drivers dramatically avoid areas near the bridge and gradually return, it is proposed that an additional perceived cost exists as a result of the disruption. Applying the calibrated mesoscopic simulation model suggests that this perceived cost evolves as an exponential decay function and is found to be relatively lower as the distance farther away from the event site. We validated the exponentially decreasing perceived cost in the mesoscopic simulator, which influences route choice in such a manner that the simulated demand falls within an acceptable error range of the real demand.

7 Future Research

7.1 Integration with Microscopic Traffic Simulation Model

As discussed before, mesoscopic traffic simulation—in terms of realism—can be best described as being situated between the macroscopic traffic simulation and the detailed microscopic traffic simulation. Despite this, it can never be as accurate as a perfectly calibrated microscopic traffic simulation model for the same network. This is simply due to the fact that microscopic traffic simulation can capture finer details along a given link or intersection. The key to remember though is that this is only applicable to perfectly calibrated microscopic traffic simulation models, as microscopic traffic simulation models are difficult and time-consuming to calibrate.

One means of assistance the mesoscopic traffic simulation model can provide is knowledge of route choice behavior. Since individual vehicles can be traced, their routes can be recorded into a database. This database can be imported into a microscopic traffic simulation model and these routes can be reproduced at a microscopic level. It is important to note that such integration is important to the success of a microsimulation model, as determining path flow from an origin to a destination is critical for a microsimultion. It becomes even more important when traffic congestion spread beyond the modeling region of a microsimulation model. Under these scenarios, path flow information from a regional model will be valuable from a mesosimulation model and the finer details of traffic dynamics can be captured using micrsimulation.

With future applications of AIMSUN, a hybrid model may someday be available. Should such an application be developed, it would be highly recommended to combine features of both mesoscopic and microscopic traffic simulation to elements that do not require detail and elements that do, respectively. The extents of such incorporations are left to future work.

7.2 Integration with Day-to-Day Learning Process

To date, there is little understanding about traffic dynamics following a prolonged, unexpected network disruption. Nonetheless, it is important for practitioners and researchers to understand driver behavior after the occurrence of such events so that the resulting traffic demand can be better dealt with. In the future, we may consider integrating drivers' day-to-day learning process into the mesosopic simulator by modeling perceived cost evolution following an exponential decay function as we have tested in this work. This work may be also applicable to a wide variety of areas, primarily for unexpected network disruption.

The integration of day-to-day learning process will be useful to both practitioners and researchers in the future. For practitioners, it offers a better understanding of how traffic behaves after a tragic, unplanned disruption and a means to estimate the magnitude of the avoidance phenomenon. Such understandings would allow for more educated resource deployment to improve capacity, efficiency, and safety. For researchers, it offers a simple concept behind the traffic dynamics following this type of network disruption, from which more complex research in route-choice model development can be conducted. From a policy perspective, this knowledge could aid in better identifying the risks and rewards of network restoration following an unexpected tragedy. From an operations perspective, this knowledge could help traffic managers understand how traffic is evolving in the long-term and the dynamics of how it will get there.

Lastly, from a safety perspective, this knowledge could provide insight of where network congestion may appear, allowing a more effective deployment of incident management resources and infrastructure improvements.

References

1. Bell, M.G.H. 1991. “The estimation of origin-destination matrices by constrained generalized least squares.” *Transportation Research B*, 25, pp. 13-22.
2. Ben-Akiva, M., Koutsopoulos, H.N., Mishalani, R., Yang, Q. 1997. “Simulation Laboratory for Evaluating Dynamic Traffic Management Systems.” *ASCE Journal of Transportation Engineering*, 123 (4), pp. 283-289.
3. Bush, B.W. 2000. *An Algorithmic Overview of TRANSIMS*. Report LA-UR-99-7/2800, Los Alamos National Laboratories, Los Alamos, NM.
4. Cascetta, E. 1984. “Estimation of origin-destination matrices from traffic counts and survey data: A generalized least squares estimator.” *Transportation Research B*, 18, pp. 289-299.
5. Dowling, R., Holland, J., Huang, A. 2002. *California Department of Transportation Guidelines for Applying Traffic Microsimulation Model Software*, Dowling Associates, Inc.
6. Jayakrishnan, R., Mahmassani, H.S., Hu, T.Y. 1994. “An Evaluation Tool for Advanced Traffic Information and Management Systems in Urban Networks.” *Transportation Research C*, 2(3), pp. 129-147.
7. Law, A.M., Kelton, W.D. 1991. *Simulation Modeling and Analysis*. Second Edition. New York: McGraw-Hill International Editions.
8. Leonard, D.R., Power, P., Taylor, N.B. 1989. *CONTRAM: Structure of the model*. TRL Report RR 178, Transportation Research Laboratory, Crowthorn, United Kingdom.
9. Transportation Simulation Systems. 2009. *AIMSUN 6.1 User’s Manual*. Barcelona, Spain.
10. Spiess, H. 1987. “A maximum likelihood model for estimating origin-destination matrices.” *Transportation Research B*, 21, pp. 395-412.
11. Van Zuylen, H.J., Willumsen, L.G. 1980. “The most likely trip estimated from traffic counts.” *Transportation Research B*, 14, pp. 281-293.
12. Yang, H., Iida, Y., Sasaki, T. 1992. “Estimation of origin-destination matrices from traffic counts on congested networks.” *Transportation Research B*, 26, pp. 417-434.